

# Ocean Color Products in the Presence of Cirrus Cloud Contamination

February 20, 2009

Gerhard Meister, Bryan Franz,  
NASA Goddard Space Flight Center , Code 614.2, OBPG  
(Gerhard.Meister@nasa.gov, 301-286-0758, bryan.a.franz@nasa.gov, 301-286-5429)

## 1 Abstract

This memo describes how cirrus clouds as detected by the 1380nm channel affect the MODIS Aqua ocean color products. Two different approaches are used: the first approach is to correlate variations in the ocean color products to the reflectance of the 1380nm channel. The second approach uses a global level 3 dataset, and compares the ocean color products after masking for cirrus clouds to the standard processing. Both approaches produce a relatively low number of cases that are affected by cirrus contamination. Both approaches predict a comparable effect on the global averages of the ocean color products.

## Contents

<b>1 Abstract</b>	<b>1</b>
<b>2 Introduction</b>	<b>2</b>
<b>3 Methods</b>	<b>2</b>
<b>4 Level 2 analysis: one orbit</b>	<b>3</b>
<b>5 Level 2 analysis: selected granules</b>	<b>3</b>
<b>6 Global Analysis of 8 day Level 3 Data</b>	<b>4</b>
<b>7 Simulation of random masking</b>	<b>4</b>
<b>8 Global Analysis of monthly Level 3 Data</b>	<b>5</b>
<b>9 Discussion and Conclusions</b>	<b>7</b>

## 2 Introduction

Cirrus clouds are ice clouds at a very high altitude. At 1380nm, light is absorbed very effectively by water vapor. Light at that wavelength coming from the earth or even from low cumulus clouds does not reach

a sensor orbiting at an altitude of 700km. However, there is very little water vapor above cirrus clouds, so these clouds appear bright at 1380nm[2]. This memo investigates whether using the 1380nm channel could improve ocean color products.

The MODIS on Aqua has a 1380nm channel (band 26)[1]. The MODIS cloud mask (filenames starting with MYD35) contains 2 bits that use the 1380nm channel to detect cirrus clouds. The MODIS cloud products (filenames starting with MYD06) contain a separate cirrus reflectance flag which could also be used. The MODIS cloud products also contain the cirrus reflectance as a level 2 product, which is the modeled cirrus reflectance for the visible spectrum[3].

The MODIS cloud mask flag uses a range of the reflectance at 1380nm from 0.005 to 0.035 as indicator for cirrus. The same definition of a cirrus cloud is used in this memo.

### 3 Methods

In sections 4 and 5, the ocean color products are plotted versus the cirrus reflectance for the visible spectrum. This is done on a per level 2 granule basis for all granules from one orbit in section 4, for selected granules with strong cirrus contamination in section 5.

The intent is to see whether there is a trend of the ocean color products with increasing cirrus reflectance. The only expected trend is an increase of the AOT at 869nm ( $\tau_{869}$ ). Any other trend (except for the aerosol type products, e.g. Angstrom coefficient) would be interpreted as a contamination of the ocean color retrievals by cirrus clouds.

Unfortunately, one orbit of data may not be enough data to extract statistically relevant trends with this method (and my prediction is that a whole day will not be enough either). A simple example that would render this method useless is if there is an increase of the true values of the ocean color product from north to south, and an increase of cirrus clouds from north to south. In this case, scatter plots would show a trend, but it would not be a sign of a problem due to cirrus clouds.

In an attempt to improve the method, the ocean color products were divided by their median value (calculated for each pixel as the median of a 51x51 box surrounding the pixel). Then the ratio of the pixel values divided by their median was plotted versus cirrus reflectance. Even with this improvement, the data used here may be too limited, but a whole day of data could be sufficient.

A different type of analysis is applied in section 6: all level 2 granules from an 8 day period are processed to a level 3 file (4.5km spatial resolution), with and without masking for cirrus clouds on the level 2 granules. We used the cirrus cloud flag (bit 9) of the MODIS cloud mask produced by the MODIS atmosphere group (filenames starting with MYD35). The cirrus cloud flag is set when the 1380nm reflectance is between 0.005 and 0.035. The two resulting level 3 files (with and without masking for cirrus) were compared. Following a suggestion by Bo-Cai Gao, the same analysis was repeated for a monthly level 3 file, see section 8.

The analysis method applied to the level 2 granules (product divided by mean versus cirrus reflectance) was also applied to the monthly level 3 file. The median for a bin was calculated by selecting the 100 closest bins to that bin (note that 100 bins with an area of 4.5km x 4.5km cover about the same area as 51 x 51 1km<sup>2</sup> pixels, 2025km<sup>2</sup> versus 2601km<sup>2</sup>).

## 4 Level 2 analysis: one orbit

The granules used and their cirrus contamination are provided in table 1. The corresponding orbit (July 3rd 2003, over Pacific Ocean) is shown in Fig. 1. The percentage of cirrus contamination was calculated two ways: first for the whole image, then only for the valid ocean color retrievals (after masking with standard flags for L3 processing, and excluding 25 frames from each edge of the granules, which was needed to calculate the median consistently).

The granules A20031842100, A20031842110, and A20031842120 have a meaningful percentage of cirrus contamination of valid ocean color retrievals, so the analysis will focus on these granules.

Table 1 also provides the number and share of cirrus contaminated ocean color retrievals where the cirrus reflectance is larger than 0.01 and less than 0.035. It can be seen that in the most contaminated granule (A20031842100), 1.3% of the ocean color retrievals have a cirrus reflectance in that range. Fig. 1 also contains a true color image of the granule, there is a lot of cloud cover in that granule.

The scatterplot of nLw 412nm versus cirrus reflectance for A20031842110 is shown in Fig. 2. It can be seen that the unnormalized values (top left plot) do not show a consistent response to an increase in cirrus reflectance. However, after normalizing to the median (top right plot), it can be seen that there is no significant trend for the nLw when the cirrus reflectance increases. A similar conclusion can be reached for the nLw at 551nm (bottom two plots).

A similar conclusion can be drawn for 412nm from granule A20031842110, see Fig. 3. At 551nm, there seems to be a downward trend, see bottom right plot. One problem here is that the cloud shadow algorithm masks all pixels with nLw 551 values less than 0.15 (which can be seen clearly in the bottom left plot), which may influence the results.

The granule A20031842120 has less than 1% of its ocean color retrievals affected by cirrus clouds. The trend for the 551nm data after dividing by the median (bottom left in Fig. 4 shows both a trend sideways and a smaller number of pixels trending down).

Figures 5, 6, 7, and 8 show the scatterplots of most of the remaining ocean color products and SST for the granule with the highest percentage of cirrus affected ocean color retrievals. It can be seen that there is no trend for 443nm and 488nm, a trend similar to 551nm for 531nm, a very strong trend for 667nm, a trend for chlorophyll, and a significant trend for SST (looking at the normalized plots for each quantity). The AOT shows a trend in the unnormalized plot, as expected.

The scatterplots for 667nm and SST are also shown for granule A20031842110 (second highest occurrence of ocean color retrievals contaminated by cirrus, see table 1) in Fig. 9. The trend for 667nm is much less clear, the trend for SST is still present.

## 5 Level 2 analysis: selected granules

Bo-Cai Gao suggested to use the granules of table 2 for the analysis described above. They generally contain a higher percentage of cirrus pixels than the granules of the orbit chosen above. The resulting plots are available at <http://oceancolor.gsfc.nasa.gov/ANALYSIS/cirrus/global/index.html>, and are not specifically discussed in this memo. Overall, the results are very similar, the ocean color products usually did not show a strong correlation to cirrus reflectance, only in a few cases (e.g. for granule A20081101655) there is again a downward trend for the longer wavelengths.

Granule A2008108155000 has a particular high number of ocean color retrievals contaminated by cirrus (almost 24,000), so the scatter plots are shown in Figures 10-12. There are a few low outliers for 551nm and chlorophyll, but 667nm does not show a trend.

## 6 Global Analysis of 8 day Level 3 Data

The choice of which 8 day period to use was based on the level 3 cirrus reflectance maps. Another consideration was to maximize coverage at both northern and southern high latitudes, so March and September were preferred. The period chosen was days 81 to 88 of the year 2007, the corresponding level 3 cirrus reflectance map is shown in Fig. 13. For the purpose of this study it would have been preferable to base the choice on variability of cirrus reflectance (with day-to-day variations of 1380nm reflectance from 0 to 0.035 being preferred), but such a map was not available.

Global maps of the results and the differences are shown at <http://oceancolor.gsfc.nasa.gov/ANALYSIS/cirrus/global/index.html>. It is possible to zoom into the images on the website, which is an advantage over the images in this memo.

It is almost impossible to see any difference (except for coverage issues) between the global absolute result maps, so this memo only shows the relative difference maps (Figs. 15 to 19). The color bar is shown in Fig. 14.

It can be seen that there are large parts of the ocean where no change at all has occurred, or the change appears randomly positive or negative. But there are certain areas (see e.g. the red area west of the coast of Chile) where a contiguous region has consistently higher nLw in the cirrus masked data than in the baseline. This area is shown enlarged in Fig. 16.

Table 3 shows some statistics for the global analysis. Overall, there is a clear bias in the nLw at 412nm and at 551nm. There are about twice as many bins in the cirrus masked data set where the nLw has increased by more than 5% than where the nLw has decreased by more than 5%. It is not quite clear how much of these changes should be attributed to noise, but it seems likely that the higher occurrence of increases than of decreases is not due to noise, but due to the cirrus clouds. So cirrus contamination seems to lower the nLw for 412nm and 551nm. This result was also found in section 4 for some granules for 551nm, but not for 412nm.

The effect on chlorophyll is less significant (a change of 10% in chlorophyll concentration is less important than a change of 10% in nLw at 412nm or 551nm). There is a clear bias in AOT: as expected, there are many more occurrences of decreased AOT in the cirrus-masked product.

Fig. 20 shows the histograms of those changes larger than 5%. It can be seen that the histograms are smooth functions.

The bins were averaged into 5deg latitudinal zones. The averages and the differences are shown in Fig. 21 for the 8 day level 3 file. For the 412nm nLw, the difference between cirrus-masked and baseline is less than 1%, except for the highest latitude zone (70°-75°), where the number of bins probably dominates the result (there are 5700 bins in the zone 70°-75° in the baseline level 3 file versus only 4800 bins in the cirrus-masked level 3 file). The nLw at 551nm are biased low by about 0.5% for most latitudes, for 667nm the nLw are lower from 0 to 3%. The chlorophyll differences vary from -3% to +1%.

## 7 Simulation of random masking

Any significant change in masking will produce a change in the level 3 products. In the following, we will present a simulation of this effect, starting from global level 3 daily products.

The simulated products shall have a mean value of 100 for every bin. A 10% standard deviation noise will be added to the data. The baseline product shall be masked randomly with a 50% chance of cloud cover. This means that the baseline 8 day level 3 bin will be calculated as the average of 0-8 values. The new-mask product starts with the same noised up data as the baseline product. It adds a 6% random

masking on top of the 50% cloud mask from the baseline to simulate a change in masking, e.g. due to cirrus clouds. The new-mask 8 day level 3 product is calculated from the newly masked daily level 3 product.

The histogram of the difference between the baseline product and the new-mask product is shown in Fig. 22. About 5% of the 8-day level 3 bins have a change of more than  $\pm 5\%$ . It can be seen that the distribution is symmetric around 0.

This simulation shows that any masking change will produce a change in the level 3 products. However, it does not show how much of a change should be expected, because the assumptions (50% random cloud cover, 10% standard deviation for daily observations) are first guesses. E.g., assuming a 5% standard deviation for the daily observations leads to 0.8% of the bins having a change of more than  $\pm 5\%$ .

The results from this simulation could be applied to the results of section 6 as follows: we do not know what percentage of the histograms shown in Fig. 20 is due to sampling issues due to additional masking. However, the assymetry between the increases and decreases (e.g. the cirrus masked products clearly show a larger incidence of increased nLw) should be due to the radiometric effect of cirrus cloud contamination.

Potential shortcomings of the simulation are:

- It does not start on L2 granules, but on daily L3 bins.
- Assumed values (10% standard deviation of daily values, 50% cloud cover) may be off.
- Distributions are unlikely to be random (e.g. cloud cover could be highly localized).
- Sampling at the high latitudes is higher than at the equators in reality, but not in the simulation.

The choice for 6% additional random masking in the simulation was based on the fact that 3% of the bins were lost in section 6 in the cirrus-masked 8-day level 3 compared to the baseline. This means that in the dailies, the cirrus masking must have been higher than 3%, a first estimated was twice as high, which seems realistic when compared with the share of ocean color retrievals contaminated by cirrus given in tables 1 and 2.

## 8 Global Analysis of monthly Level 3 Data

The choice of the 8 day period in section 6 was somewhat arbitrary. Bo-Cai Gao suggested a month (September of 2005) that he had used in previous studies because it contains large cirrus contaminations. We repeated the latitudinal analysis of section 6 for this month (comparing ocean color products with and without cirrus masking). We did not calculate the SST product, but added several products related to the fluorescence line height (flh) product, e.g. the water-leaving radiances at 678nm and 748nm.

The results are shown in Figs. 23 and 24. It can be seen that the water-leaving radiances from 412nm to 551nm never differ by more than 1%. The nLw at 667 and 678 differ more, but this is expected due to their small absolute values. The flh product varies by only up to 3%, which is probably not significant. The chlorophyll values are within 2%. The largest cirrus contaminations are around the equator, as can be seen by the reduction in cirrus reflectance ( $\rho_{\text{cirrus}}$ ) of the cirrus masked product.

A histogram of the bins with changes larger than 5% is shown in Fig. 25. It looks very similar to the corresponding plot of the 8-day level 3 files (Fig. 20). The number of bins in the monthly level 3 is almost twice the number of bins in the 8 day level 3, so the total number of bins with changes larger than 5% is larger in the monthly level 3 as well. However, even relative to the total number of bins, the percentages of bins with more than 5% changes have increased, as can be seen in table 4.

The analysis of the level 2 granules (plotting product or product divided by mean versus cirrus reflectance) can also be done for the unmasked monthly level 3 data (but not for the weekly level 3 data, because that data set didn't contain cirrus reflectance as a product). The approach was slightly modified:

- We no longer look at the ratio to the mean, but at the difference to the mean.
- The mean is calculated as the mean product value of the 10 closest bins. If any of the 10 closest bins has a value of rho\_cirrus of more than 0.0025, it is not considered in the average. The mean is only calculated if at least 3 of the 10 closest bins have a value of rho\_cirrus of less than 0.0025.

The results are shown in Fig. 26 to 31. (Note that the plotting range for the cirrus reflectance in Fig. 26 is smaller than for the L2 granules, see e.g. Fig. 2.) It can be seen that again there is a trend in the 412nm nLw minus mean versus rho\_cirrus, but not in the longer wavelengths (e.g. at 551nm).

In order to evaluate the impact of the trend, a linear function was fitted to the difference plots, shown as a white (close to horizontal) line. The optimization equation is

$$p_0 + p_1 * \rho_i^c = product_i - mean_i \quad (1)$$

where  $p_0$  and  $p_1$  are the desired parameters of the linear function,  $\rho_i^c$  is rho\_cirrus of bin  $i$ ,  $product_i$  is the value of the ocean color product at bin  $i$ , and  $mean_i$  is the mean product value of the (up to 10) bins surrounding bin  $i$ . The assumption for eq. 1 is that the true value of the ocean color product at bin  $i$  (or rather the value if there was no cirrus present) can be approximated by the average of the surrounding pixels that have low cirrus contamination. This assumption may not be good for an individual bin, but it should be adequate after averaging over a sufficiently large number of bins.

We calculated the value of rho\_cirrus where the linear function exceeds 1% of the mean product value. This value of rho\_cirrus is shown as a vertical white line. The numerical results are provided in table 5. E.g. at 412nm, 4.4% of the bins are expected to be biased low by 1% or more. This percentage decreases with wavelength until 488nm, which has the lowest percentage with 0.6% of the bins expected to be biased low by 1% or more. The numbers increase again for the nLw of 531nm nLw and reach a maximum of 32.7% for the 678nm band, but the low absolute value of the red bands is not well suited for applying this metric (a 1% variation of the red band nLw is much less meaningful than a 1% variation at 412nm). Therefore, the same metric is provided in table 5 with a 5% threshold, the maximum share of water-leaving radiances affected more than 5% is 1.5% at 678nm.

Consistency between the results from comparing the masked and the unmasked L3 files (Figs. 23 and 24) and the linear fit derived from the scatterplot analysis was evaluated the following way: all the level 3 bins of the scatter plot analysis (or the unmasked L3 file) with rho\_cirrus greater than 0.0025 were corrected using the linear fit:

$$product_i^{corrected} = product_i - (p_0 + p_1 * \rho_i^c) \quad (2)$$

Then the global average of the product (for all rho\_cirrus) was calculated for the corrected product. The difference original product minus corrected product is shown in the last column of table 5, subcolumn labeled 'fit'. It is a measure of the expected global impact. Qualitatively, there is good agreement to the ratios shown in Figs. 23 and 24, except for the product rho\_cirrus. (The product rho\_cirrus cannot be evaluated with the scatterplot analysis, see the following paragraph.) For ease of comparison, the difference of the global average of the unmasked minus the masked ocean color products is shown in the

second subcolumn (labeled 'mask') of the last column of table 5. All the differences have the same sign (except for nLw 488 and nLw 531), the water-leaving radiances up to 551nm are all within 0.1%.

The ideal fit parameters for rho\_cirrus in table 5 would be 0 and 1.0. The retrieved offset parameter is very close to 0, but the slope parameter is 0.67, far from 1.0. The difference is most likely due to choosing only rho\_cirrus smaller than 0.0025 when calculating the mean of the surrounding bins. (Imagine a spatially homogeneous area of high rho\_cirrus; because of the selection criteria for the surrounding bins, it will not be included in the calculation of the fit parameters in eq.1. On the other hand, for an inhomogeneous area with rho\_cirrus values higher and lower than the chosen threshold (0.0025), the  $mean_i$  will be calculated only for the bins with rho\_cirrus less than the threshold, resulting in a low bias for the fit parameters.)

## 9 Discussion and Conclusions

The monthly level 3 data set is the most reliable data set used in this study, because it is based on the highest number of measurements. A decline with cirrus reflectance was found for nLw of all wavelengths when plotting the nLw product after subtracting the median versus the cirrus reflectance, see Figs. 26 to 31. However, only very few pixels are affected significantly (for nLw 412nm to 551nm, less than 5% of the bins are affected by more than 1%, less than 0.1% of the bins are affected by more than 5%). The global average of the nLw at these wavelengths is affected by less than 0.1%, see table 5.

A possible method of dealing with cirrus contamination is masking the cirrus contaminated pixels. We compared the ocean color products from the masked and the unmasked L3 files for 8-day L3 files and monthly L3 files. In the global 8-day (monthly) analysis, the number of bins in the cirrus masked data set was about 3% (2%) lower than in the baseline. Therefore, masking for cirrus would reduce coverage by 2-3%, and it would improve the radiometric quality of 0.5%-1.0% of the bins by 5% or more. This improvement is almost unnoticeable when looking at larger areas, e.g. when averaging global ocean color products as a function of latitude, see Figs.21 and 23.

The effect on the ocean color products was evaluated with two independent methods:

- Fitting a linear function to the data after subtracting the median
- Comparing the masked and the unmasked L3 files (taking into account the expected variations due to the different masking scheme)

On a global scale, the predicted effects are very comparable, see last two columns in table 5. This can be seen as an indication that the results are realistic estimates.

## References

- [1] W. L. Barnes, T. S. Pagano, V. V. Salomonson, Prelaunch Characteristics of the Moderate Resolution Imaging Spectroradiometer (MODIS) on EOS-AM1, IEEE Tr. Geosc. Rem. Sens., Vol.36, No.4, pp.1088-1100, 1998.
- [2] B. Gao, Y. J. Kaufman, W. Han, W. J. Wiscombe, Correction of thin cirrus path radiances in the 0.4-1.0 $\mu$ m spectral region using the sensitive 1.375 $\mu$ m cirrus detecting channel, Journal of Geophysical Research, Vol.103, No.D24, pp.32169-32176, 1998.

- [3] B. Gao, P. Yang, W. Han, R. Li, W. J. Wiscombe, An Algorithm Using Visible and  $1.38\mu\text{m}$  Channels to Retrieve Cirrus Cloud Reflectances From Aircraft and Satellite Data, *IEEE Tr. Geosc. Rem. Sens.*, Vol.40, No.8, pp.1659-1668, 2002.

Table 1: Cirrus contamination of granules (i.e. share of 1380nm reflectances between 0.005 and 0.035; second and third column). The number of contaminated ocean color retrievals is given in brackets. Each granule has 2.6 million pixels (after eliminating 25 pixels from the edge of each scan).

Granule	of whole image	of ocean color retrievals
A2003184210000.L2_LAC	19.6 %	1.7% (3165)
A2003184210500.L2_LAC	6.2 %	0.1% ( 430)
A2003184211000.L2_LAC	20.2 %	0.7% (1687)
A2003184211500.L2_LAC	1.4 %	0.0% ( 82)
A2003184212000.L2_LAC	8.0 %	0.2% ( 245)

Table 2: Cirrus contamination of granules suggested by Bo-Cai Gao. The number of contaminated ocean color retrievals is given in brackets.

Granule	of whole image	of ocean color retrievals
A2008108090500.L2_LAC	15.7 %	6.5% ( 7383)
A2008108155000.L2_LAC	18.4 %	4.1% (13881)
A2008108223000.L2_LAC	39.5 %	1.1% ( 564)
A2008110040500.L2_LAC	21.4 %	1.4% ( 926)
A2008110085500.L2_LAC	6.3 %	0.0% ( 0)
A2008110165500.L2_LAC	18.6 %	1.2% ( 5086)
A2008116213000.L2_LAC	16.5 %	0.2% ( 964)
A2008123164500.L2_LAC	29.1 %	0.2% ( 163)
A2008124184500.L2_LAC	14.0 %	0.7% ( 548)
A2008126183000.L2_LAC	24.6 %	2.1% ( 211)

Table 3: Statistics for the global 8-day analysis: increase and decrease of ocean color products in cirrus masked products relative to baseline product. There were a total of 7,582,215 common bins in the two level 3 files.

Product	percentage of bins (relative to all bins) with >5% decrease	median decrease of product for pixels in previous column	percentage of bins (relative to all bins) with >5% increase	median increase of product for pixels in previous column
nLw 412nm	0.9%	9.6%	1.8%	10.8%
nLw 551nm	0.7%	9.2%	1.4%	8.7%
AOT 869nm	4.3%	19.2%	1.1%	11.0%
Chlor-a	1.1%	9.5%	1.7%	9.3%

Table 4: Statistics for the global monthly analysis: increase and decrease of ocean color products in cirrus masked products relative to baseline product. There were a total of 12,901,634 common bins in the two level 3 files (with 13,144,970 bins in the unmasked file)

Product	percentage of bins (relative to all bins) with >5% decrease	median decrease of product for pixels in previous column	percentage of bins (relative to all bins) with >5% increase	median increase of product for pixels in previous column
nLw 412nm	1.7%	8.6%	2.7%	9.1%
nLw 551nm	1.3%	7.8%	2.2%	7.9%
AOT 869nm	8.9%	15.8%	2.5%	10.2%
Chlor-a	2.5%	9.6%	3.0%	8.6%

Table 5: Statistics for the global monthly analysis: expected contamination of ocean color products by cirrus clouds.

Product	Mean	Share of bins affected >1%	Share of bins affected >5%	Linear fit: offset	Linear fit: slope	Global impact fit	Global impact mask
nLw 412nm	1.71	4.4%	0.08%	0.0129289	-12.6375	-0.08%	-0.07%
nLw 443nm	1.48	1.8%	<0.01%	0.00723764	-7.02094	-0.04%	-0.02%
nLw 488nm	1.14	0.6%	<0.01%	0.00365676	-3.43416	-0.03%	+0.003%
nLw 531nm	0.487	1.3%	<0.01%	0.00240182	-2.07560	-0.04%	+0.05%
nLw 551nm	0.351	4.0%	0.07%	0.00290695	-2.61407	-0.07%	-0.07%
nLw 667nm	0.0314	30.3%	1.3%	0.000731296	-0.665124	-0.2%	-0.4%
nLw 678nm	0.0323	32.7%	1.5%	0.000788815	-0.725984	-0.2%	-0.5%
FLH	0.00511	41.6%	2.7%	0.000151329	-0.146606	-0.3%	-1.0%
Chloro-phyll-a	0.265	7.4%	<0.01%	0.00114166	0.761383	+0.06%	+0.1%
AOT 869nm	0.107	66.6%	11.0%	-0.00618974	6.69968	+0.6%	+2.1%
Epsilon	1.030	0.1%	<0.01%	0.00176685	-1.84084	-0.01%	-0.1%
Angstroem (531nm)	0.321	34.1%	2.6%	0.00840584	-8.72873	-0.3%	-0.7%
Rho_cirrus	0.00108	96.8%	84.0%	-0.000647612	0.667826	+6.0%	+21.3%

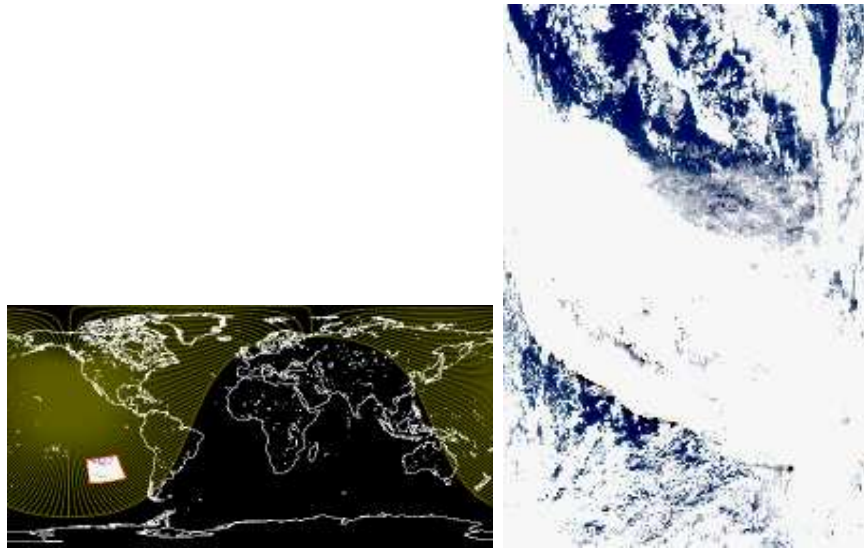


Figure 1: Left: Location of granule A20031842100. The other remaining granules of this orbit are to the north of the shown granule. Right: True color image of A20031842100.

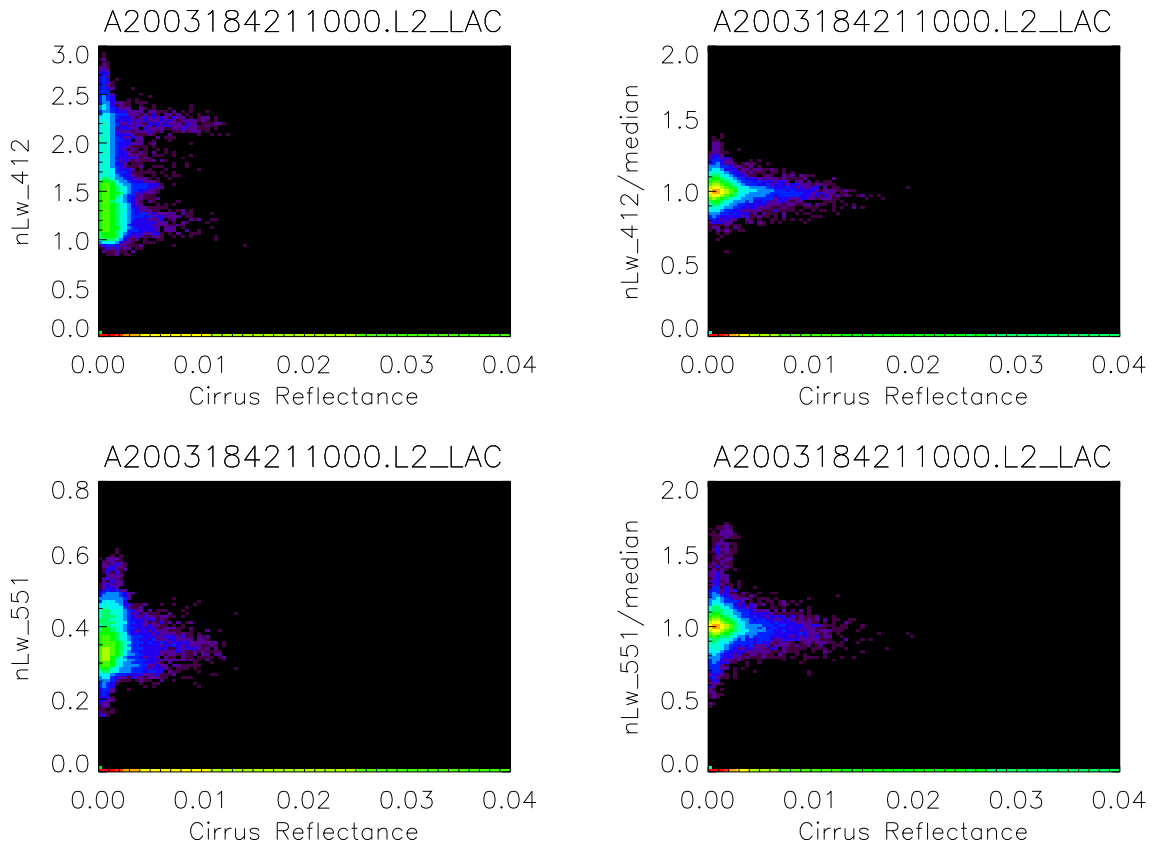


Figure 2: Scatter plot for granule A20031842110 of nLw at 412nm (top row) and 551nm (bottom row) versus cirrus reflectance, unnormalized data (left) and normalized to the median (right). The color coding is logarithmic, with purple spots being 1 pixel count.

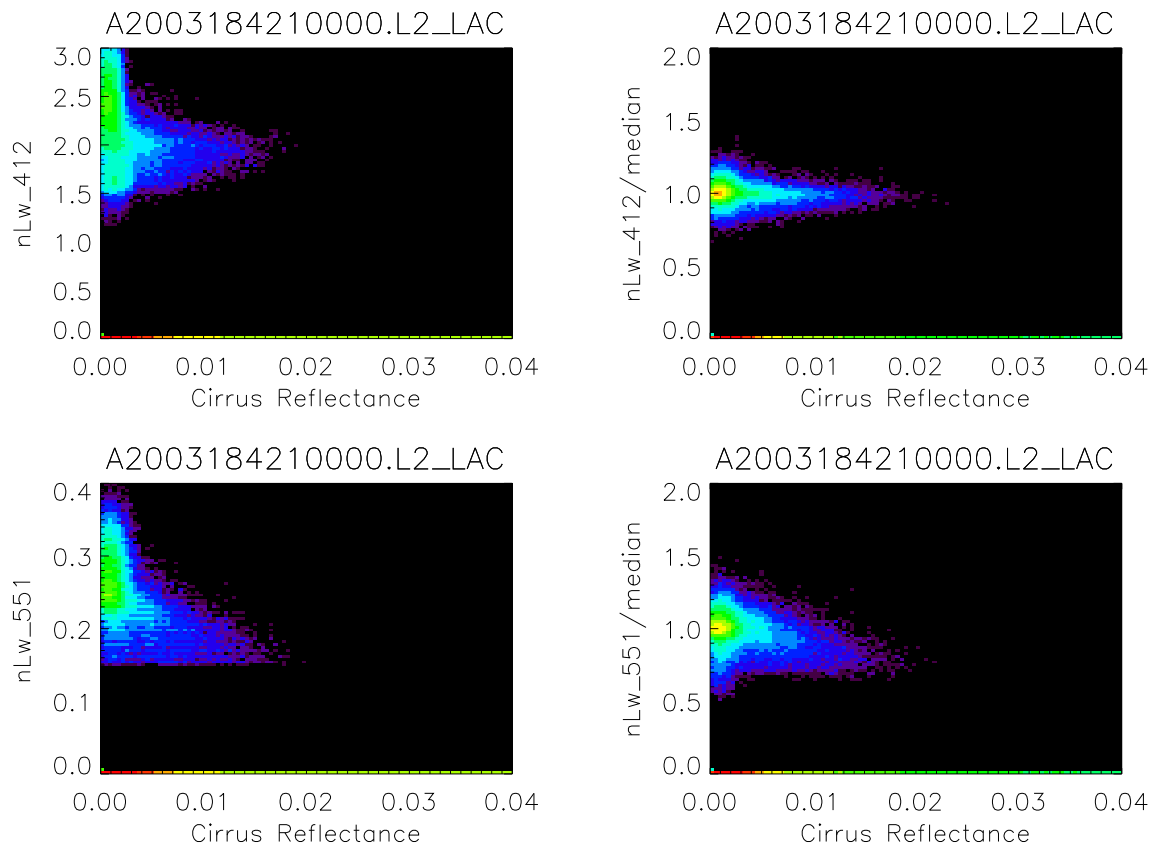


Figure 3: Scatter plot for granule A20031842100 of nLw at 412nm (top row) and 551nm (bottom row) versus cirrus reflectance, unnormalized data (left) and normalized to the median (right). The color coding is logarithmic, with purple spots being 1 pixel count.

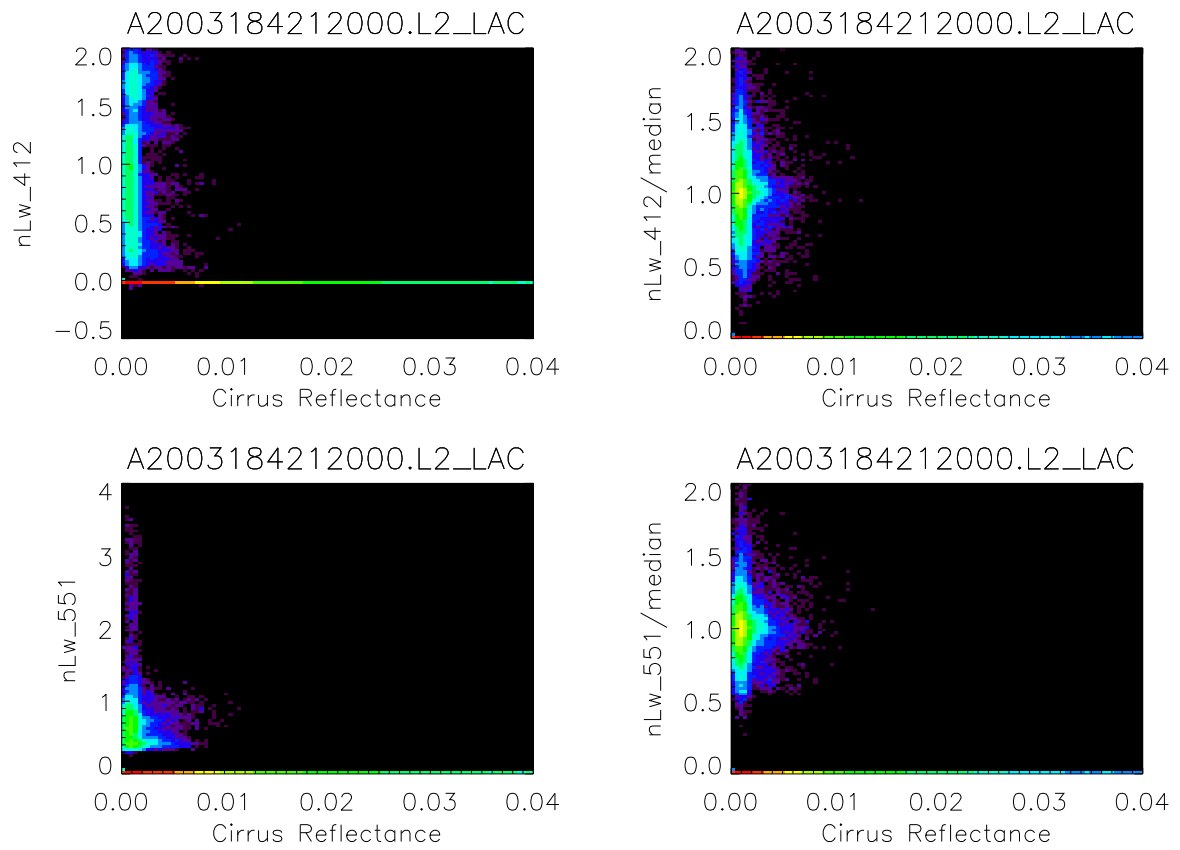


Figure 4: Scatter plot for granule A20031842120 of  $nLw$  at 412nm (top row) and 551nm (bottom row) versus cirrus reflectance, unnormalized data (left) and normalized to the median (right). The color coding is logarithmic, with purple spots being 1 pixel count.

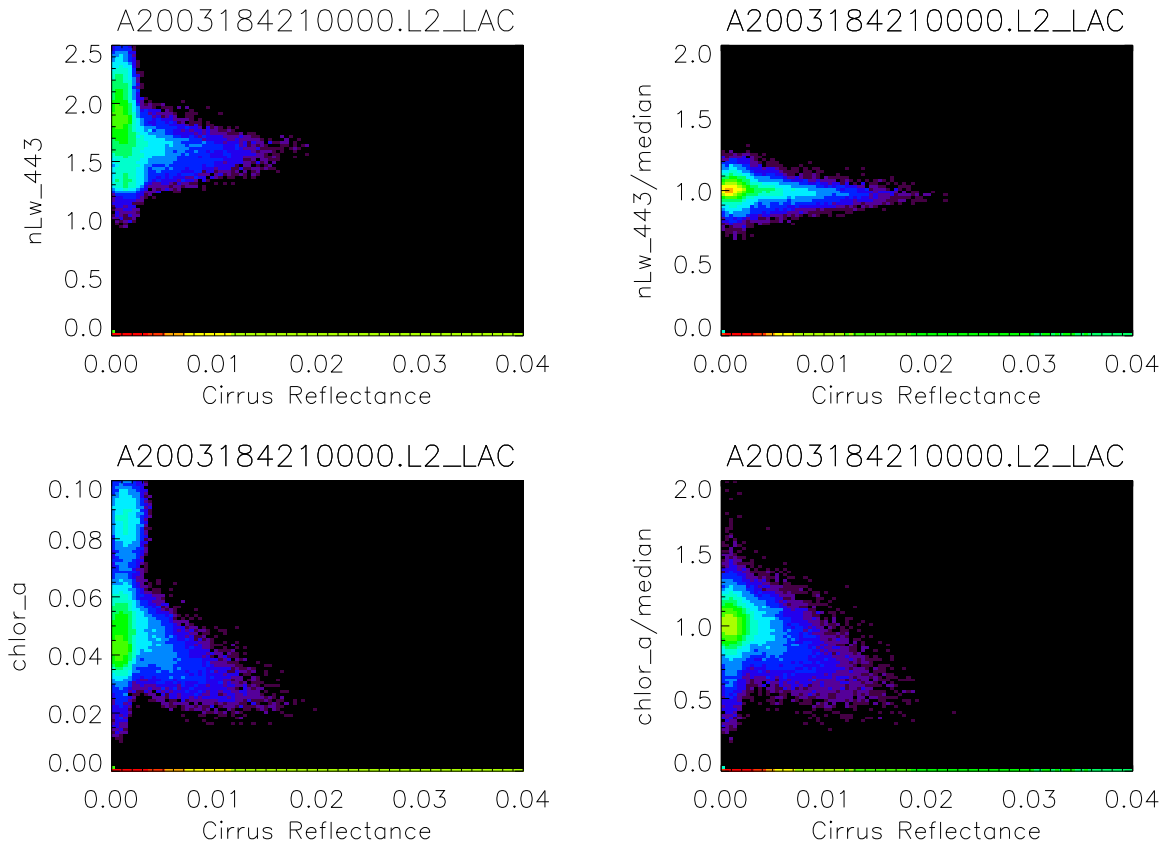


Figure 5: Scatter plot for granule A20031842100 of nLw at 443nm (top row) and chlorophyll-a concentration (bottom row) versus cirrus reflectance, unnormalized data (left) and normalized to the median (right). The color coding is logarithmic, with purple spots being 1 pixel count.

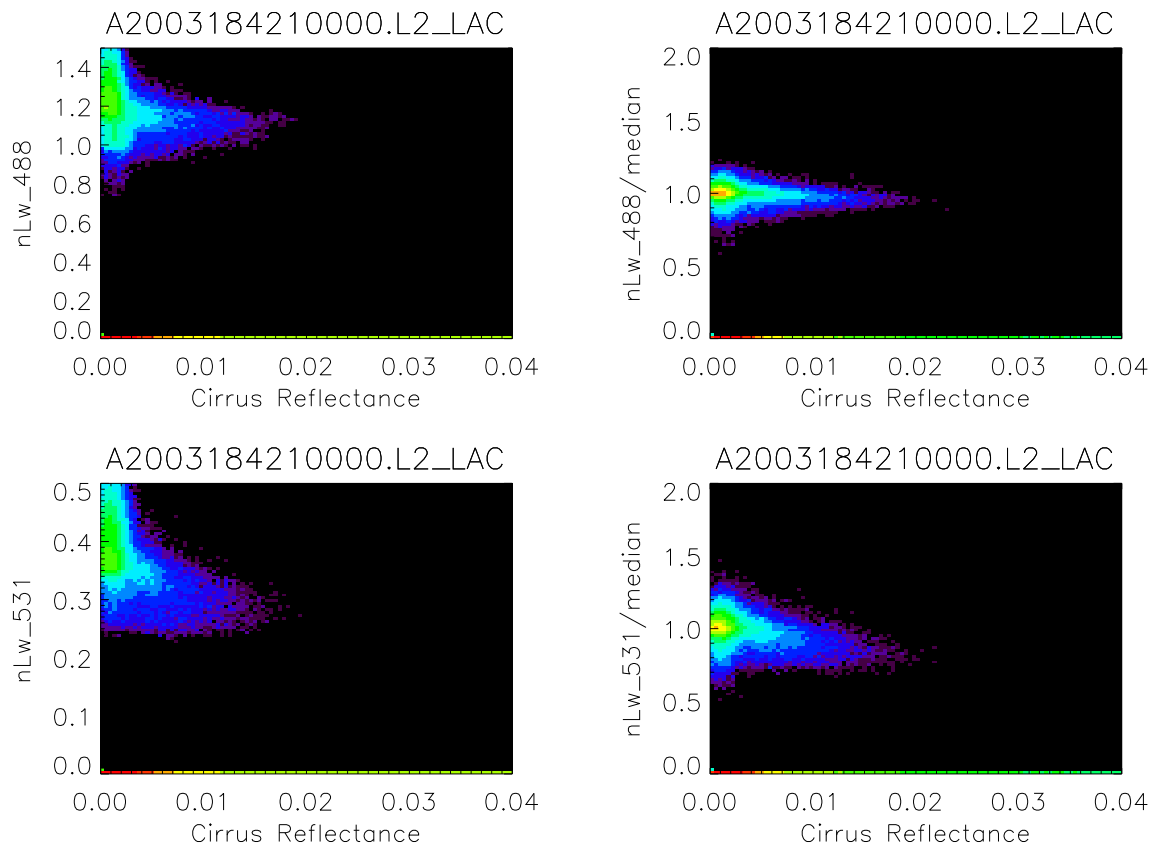


Figure 6: Scatter plot for granule A20031842100 of nLw at 488nm (top row) and 531nm (bottom row) versus cirrus reflectance, unnormalized data (left) and normalized to the median (right). The color coding is logarithmic, with purple spots being 1 pixel count.

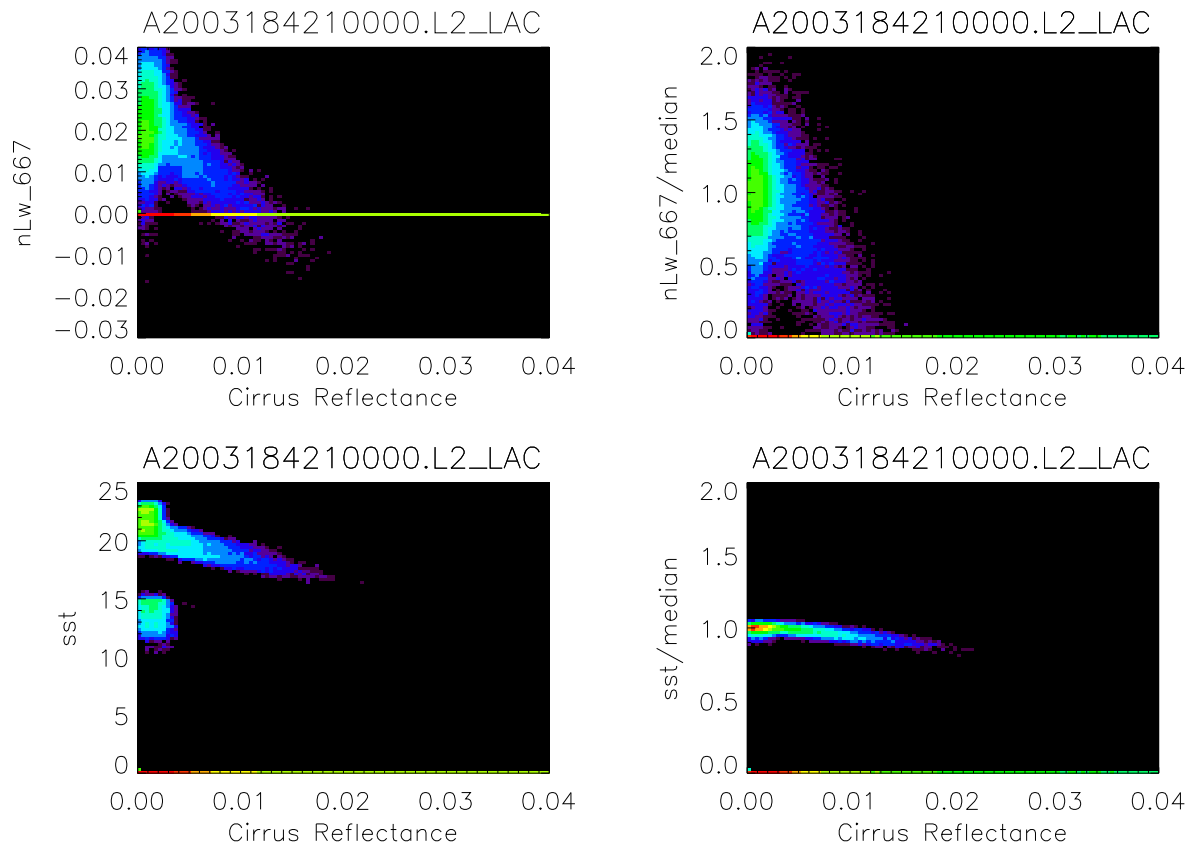


Figure 7: Scatter plot for granule A20031842100 of nLw at 667nm (top row) and SST (sea surface temperature, bottom row) versus cirrus reflectance, unnormalized data (left) and normalized to the median (right). The color coding is logarithmic, with purple spots being 1 pixel count.

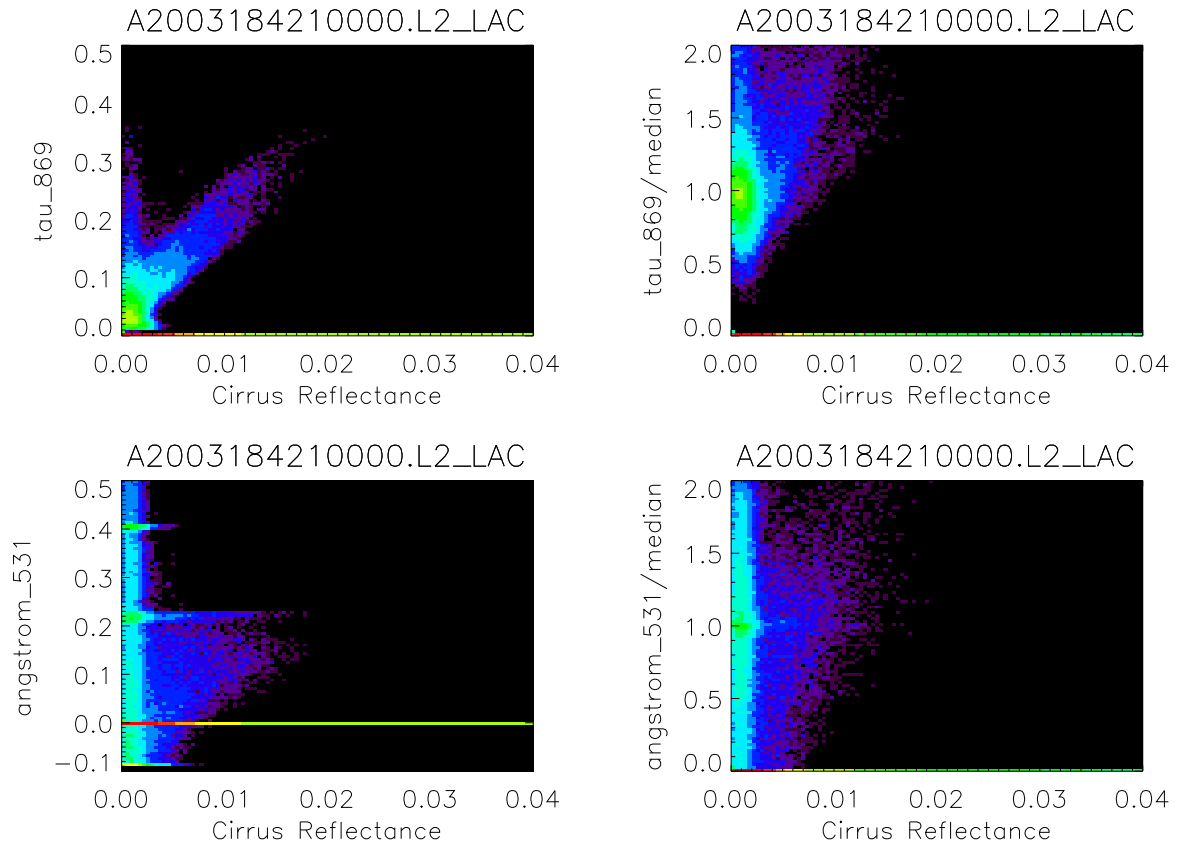


Figure 8: Scatter plot for granule A20031842100 of AOT at 869nm (top row) and Angstrom coefficient (at 531nm, bottom row) versus cirrus reflectance, unnormalized data (left) and normalized to the median (right). The color coding is logarithmic, with purple spots being 1 pixel count.

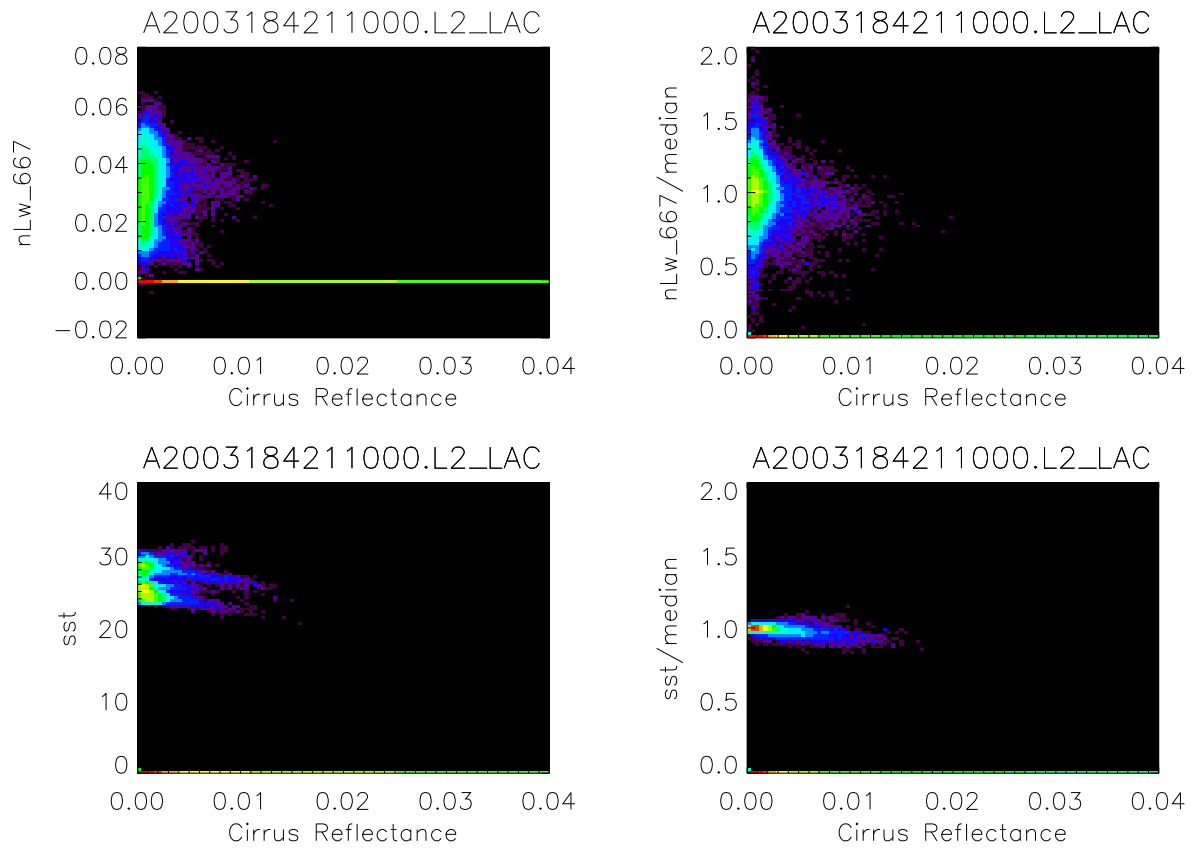


Figure 9: Scatter plot for granule A20031842110 of nLw at 667nm (top row) and SST (sea surface temperature, bottom row) versus cirrus reflectance, unnormalized data (left) and normalized to the median (right). The color coding is logarithmic, with purple spots being 1 pixel count.

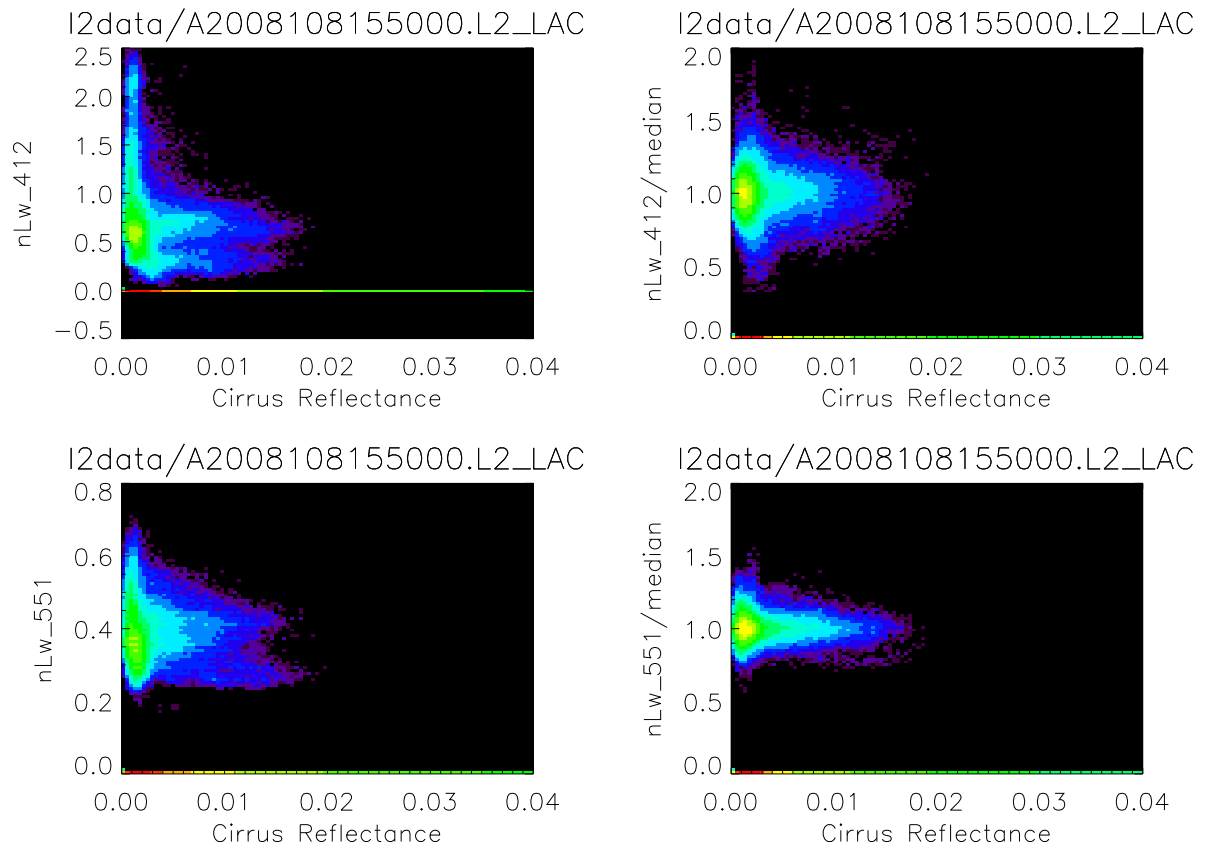


Figure 10: Scatter plot for granule A20081101550 of nLw at 412nm (top row) and 551nm (bottom row) versus cirrus reflectance, unnormalized data (left) and normalized to the median (right). The color coding is logarithmic, with purple spots being 1 pixel count.

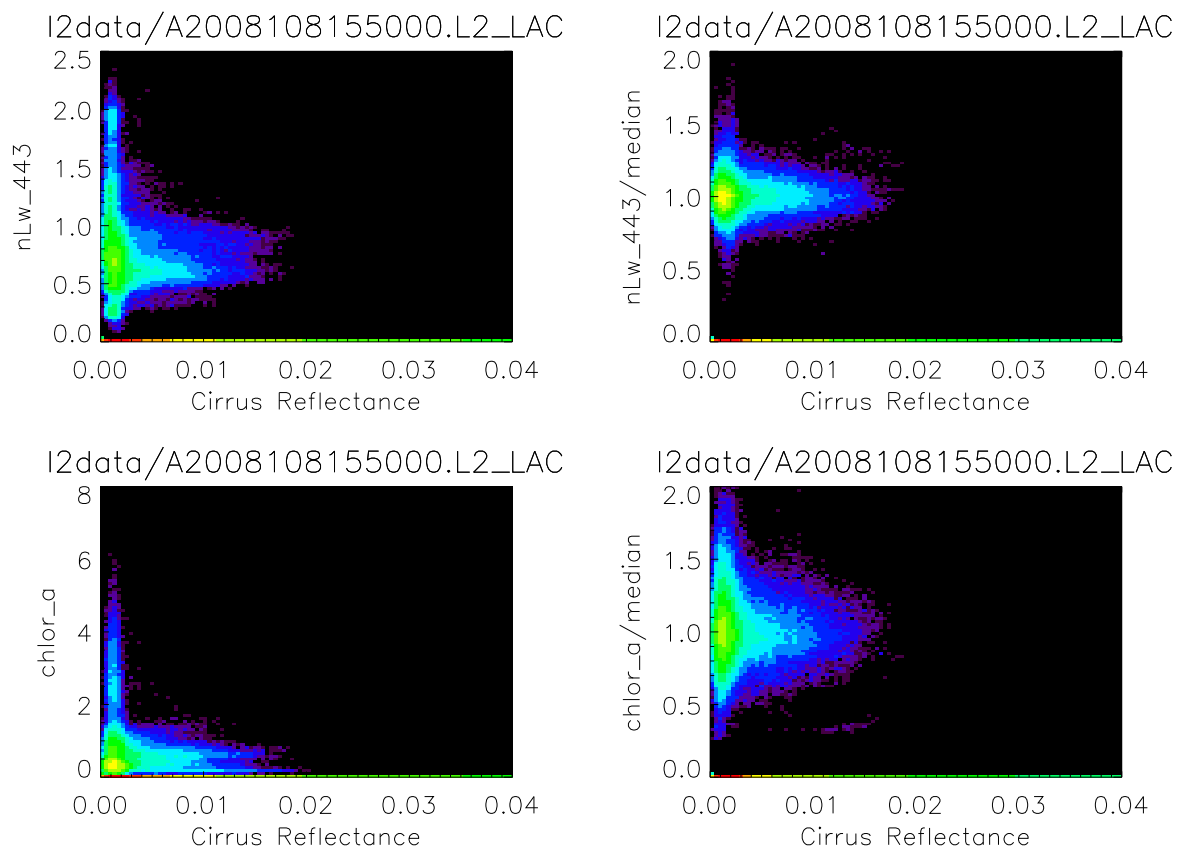


Figure 11: Scatter plot for granule A20081101550 of nLw at 443nm (top row) and chlorophyll-a concentration (bottom row) versus cirrus reflectance, unnormalized data (left) and normalized to the median (right). The color coding is logarithmic, with purple spots being 1 pixel count.

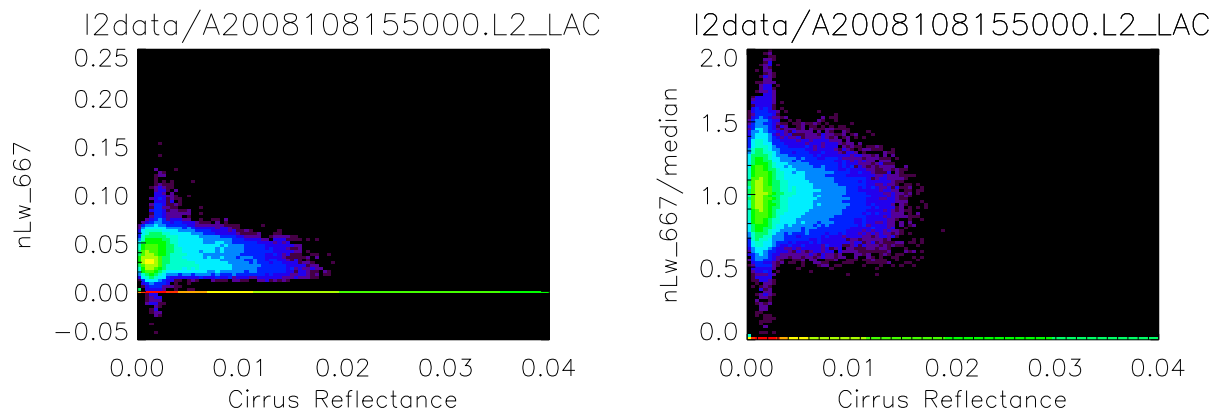


Figure 12: Scatter plot for granule A20081101550 of nLw at 667nm, unnormalized data (left) and normalized to the median (right). The color coding is logarithmic, with purple spots being 1 pixel count.

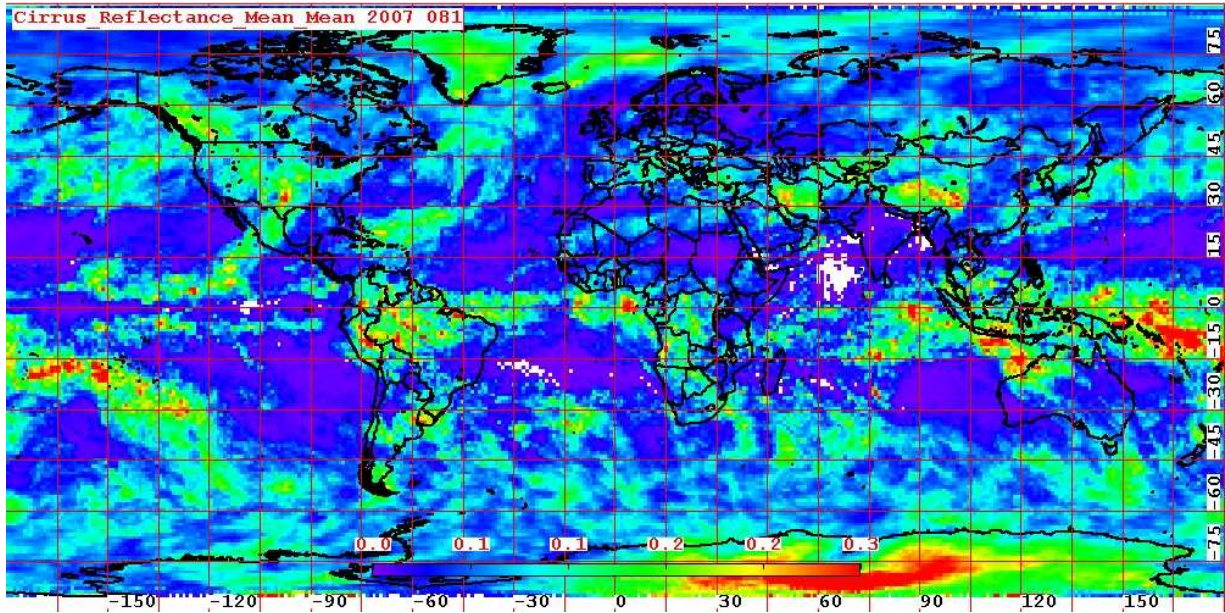


Figure 13: Level 3 8-day 1380nm reflectance for days 81 to 88 of the year 2007. The reflectance varies from 0 to 0.3 (0 to 30%). Filename as downloaded from LAADS: MYBCIR\_E3.A2007081.005.2007093063642.jpg



Figure 14: Color bar for difference images in Figs. 15 to 19. The range is -10% (purple) to +10% (red), white is no change. The difference is defined as cirrus-masked minus baseline. So the red color in the difference maps corresponds to cirrus-masked values being higher than baseline values (baseline values include the cirrus contaminated pixels, cirrus-masked do not). The black color in the images corresponds to no ocean color retrieval (usually land or persistent clouds).

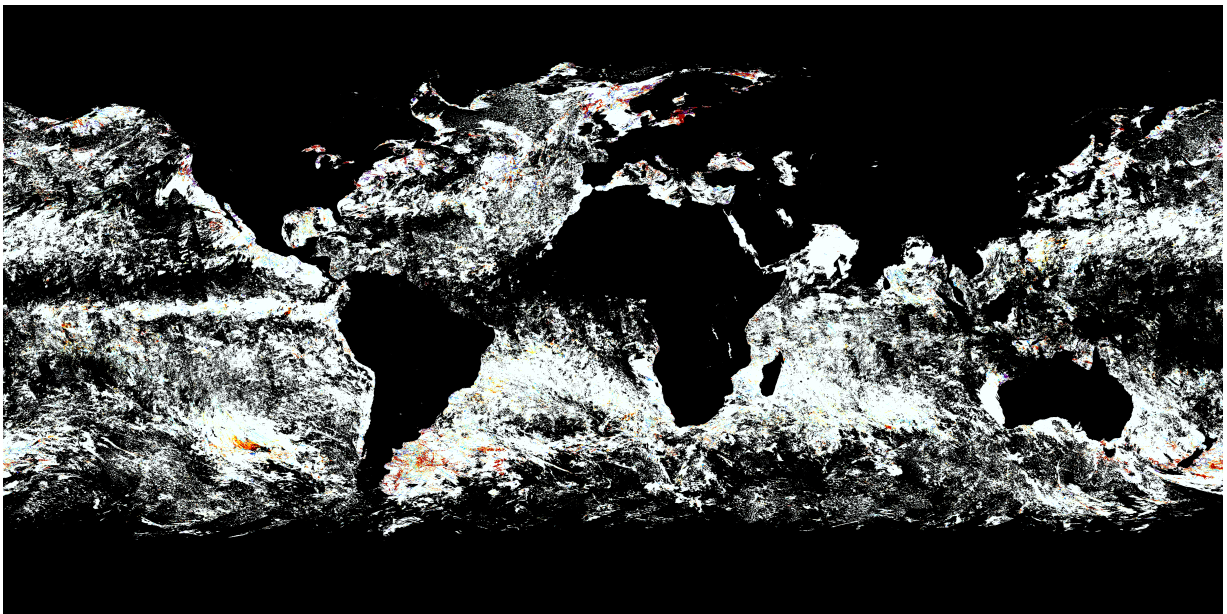


Figure 15: Global level 3 difference for nLw at 412nm. See Fig. 14 for explanations.

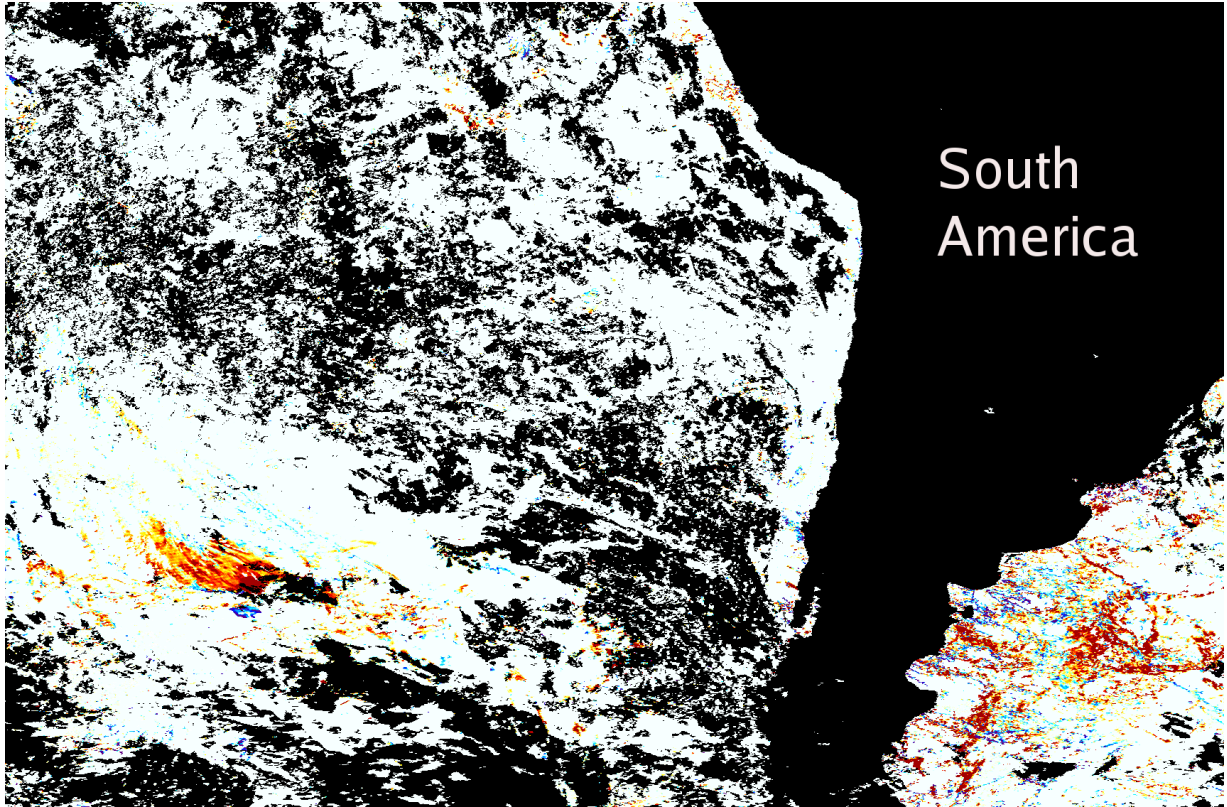


Figure 16: Level 3 difference for nLw at 412nm (South America). See Fig. 14 for explanations.

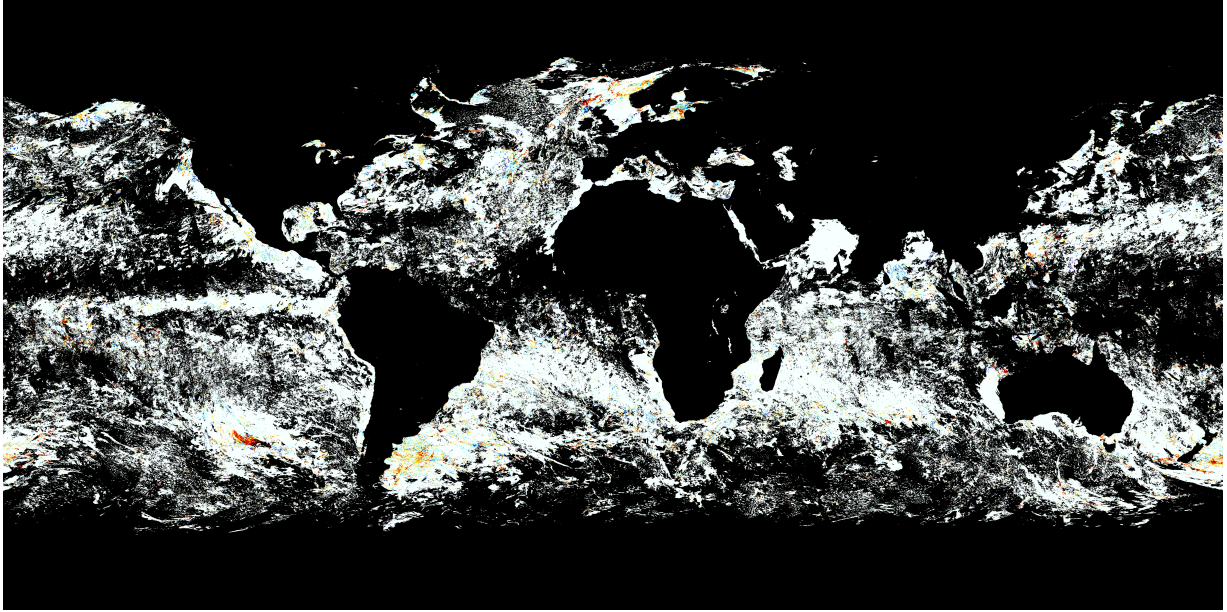


Figure 17: Global level 3 difference for nLw at 551nm. See Fig. 14 for explanations.

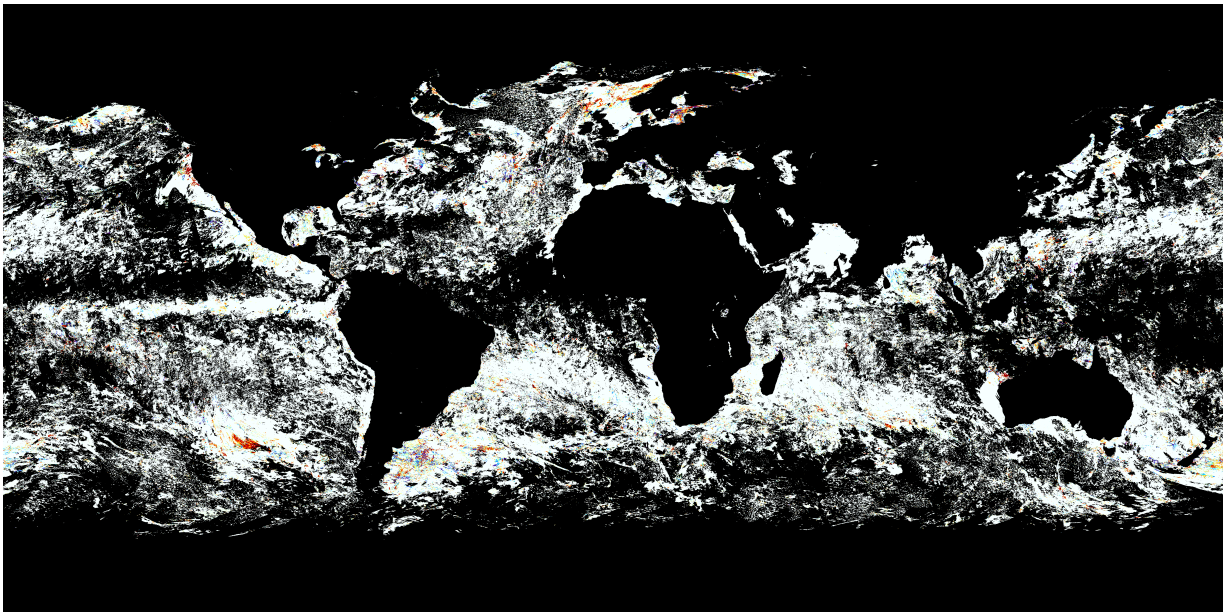


Figure 18: Global level 3 difference for chlorophyll-a. See Fig. 14 for explanations.

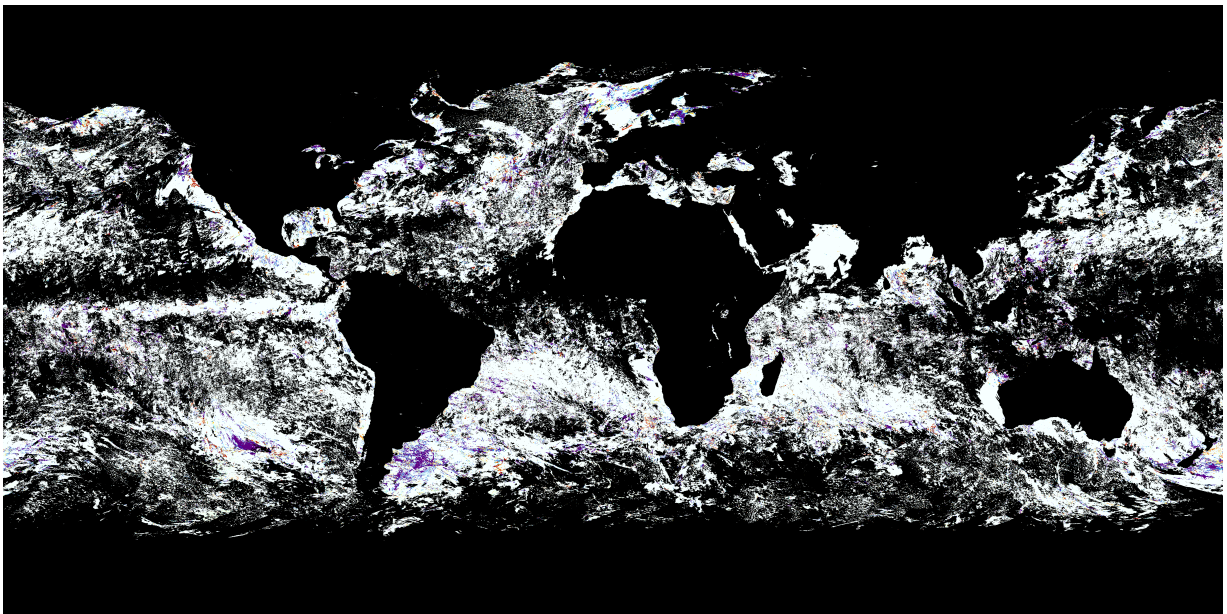


Figure 19: Global level 3 difference for AOT at 869nm. See Fig. 14 for explanations.

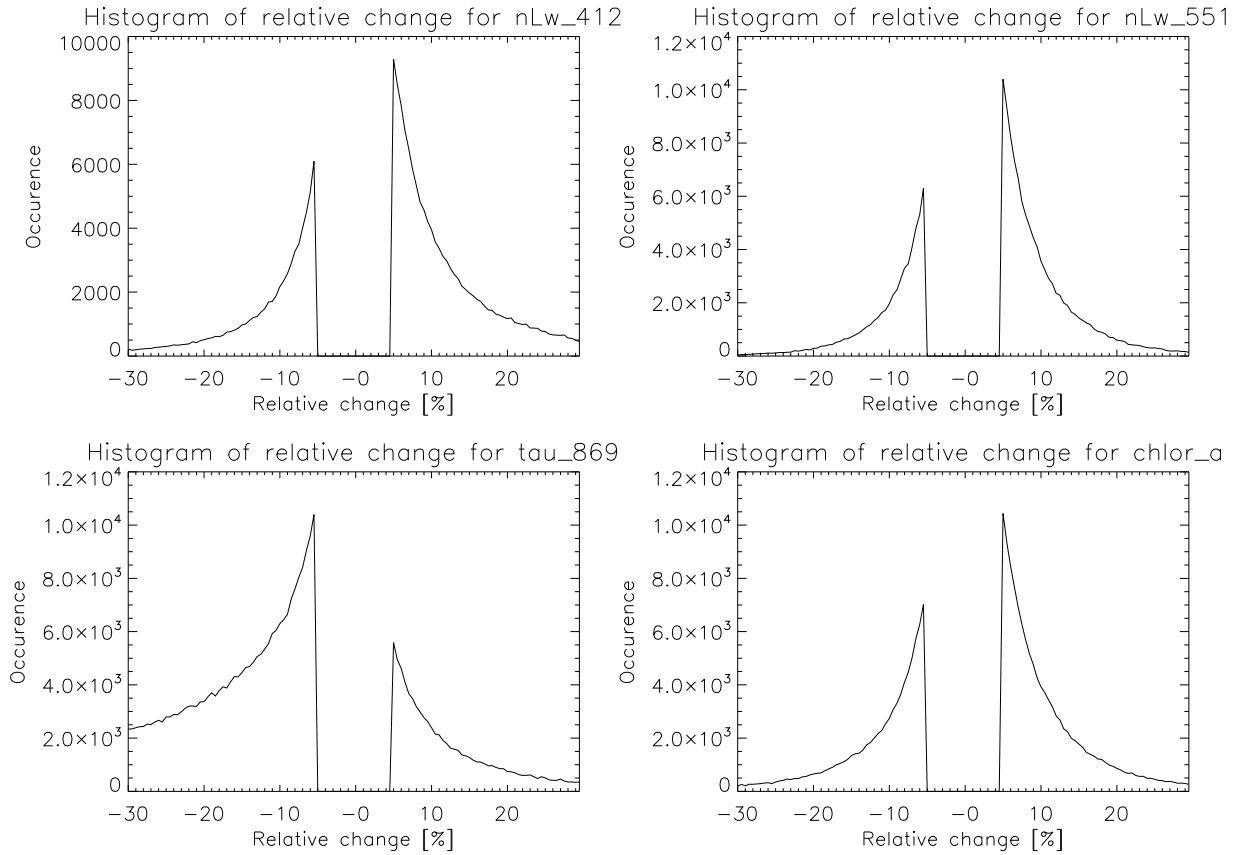


Figure 20: Histograms of the relative change (cirrus masked minus baseline) for 4 selected products from the 8-day level 3 files with absolute changes larger than 5%. Histogram-binsize is 0.5%. E.g. for nLw at 412nm, there are about 6000 bins where the nLw of the cirrus masked product is lower than in the baseline product between 5.0% and 5.5%, and about 9000 bins where the cirrus masked product is higher between 5.0% and 5.5%. The vertical lines at the  $\pm 5\%$  lines are plotting artifacts.

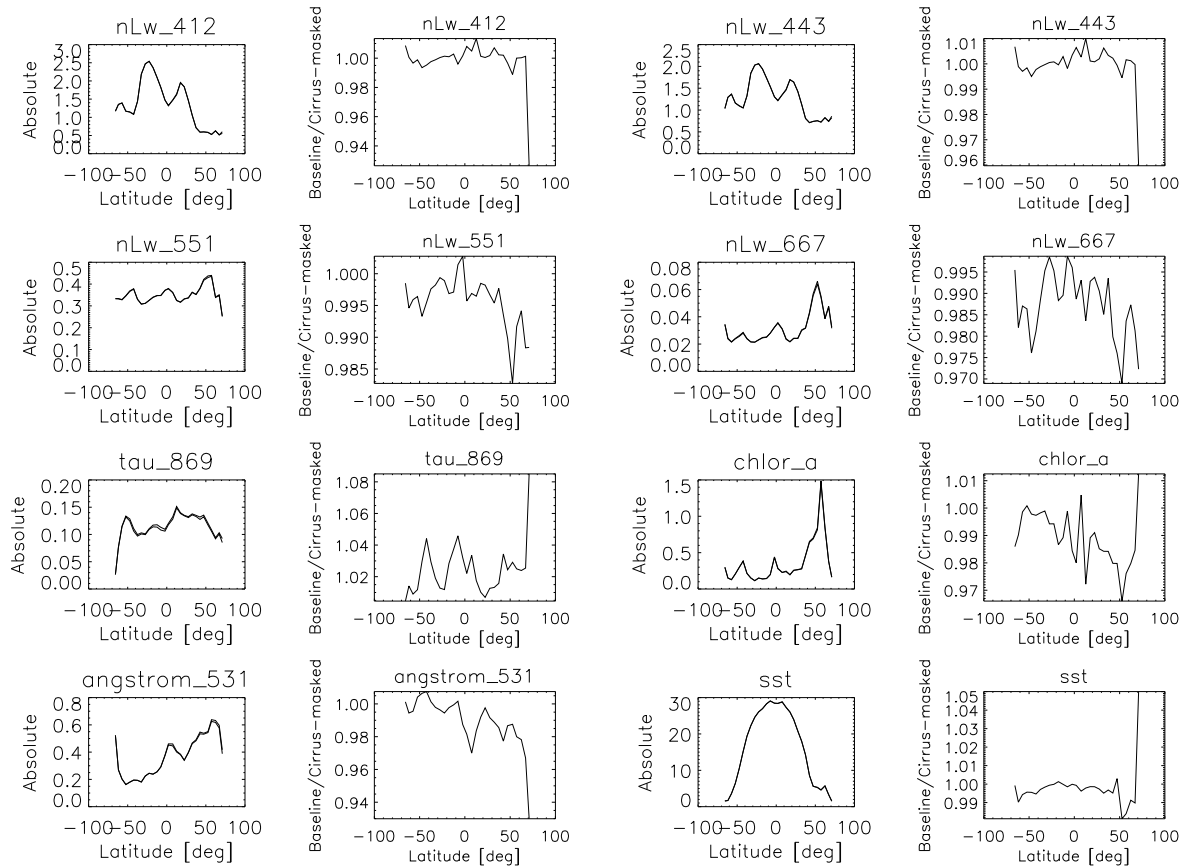


Figure 21: Different ocean products as a function of latitude, globally averaged from the 8 day level 3 file.

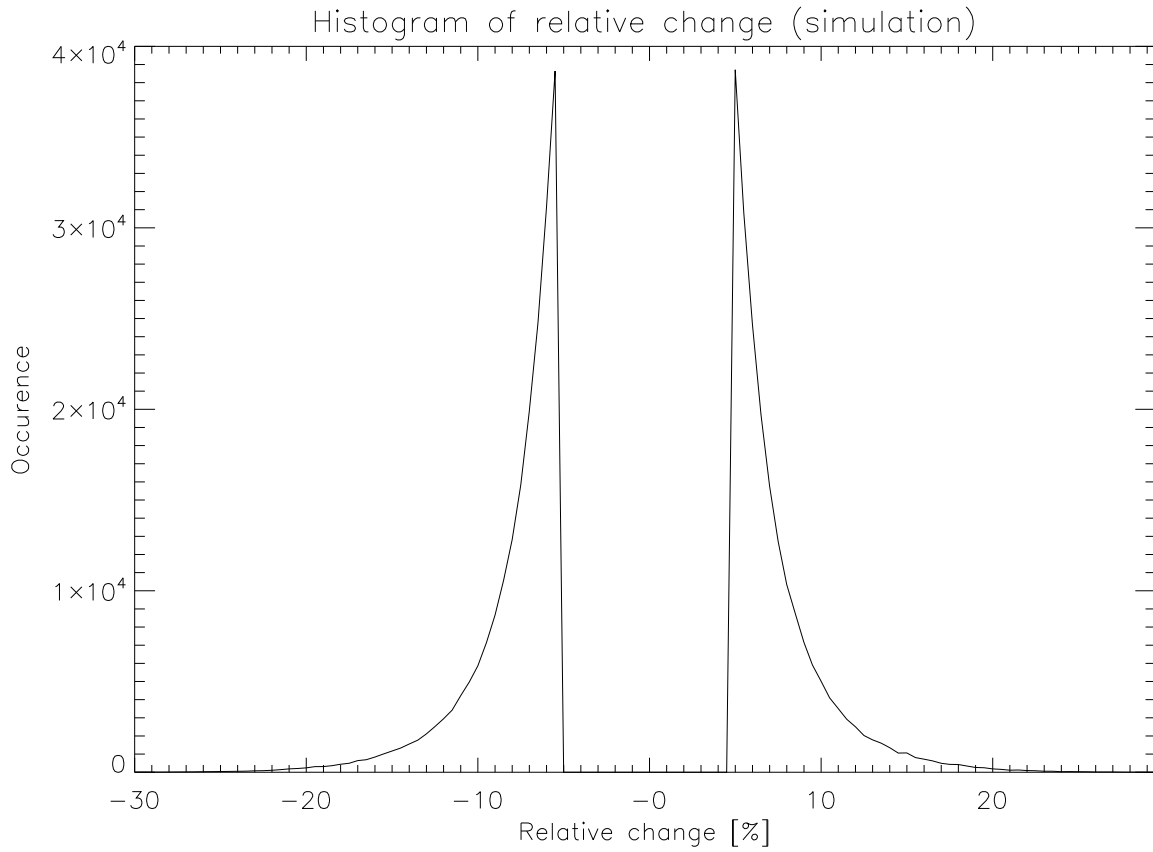


Figure 22: Histograms of the relative change (cirrus masked minus baseline) for the simulated product. The total number of bins used in the simulation is the same as in the level 3 file from section 6 (7837783), the number of bins shown above (having a difference of more than 5% between baseline masking and new-masking) is 5% of that.

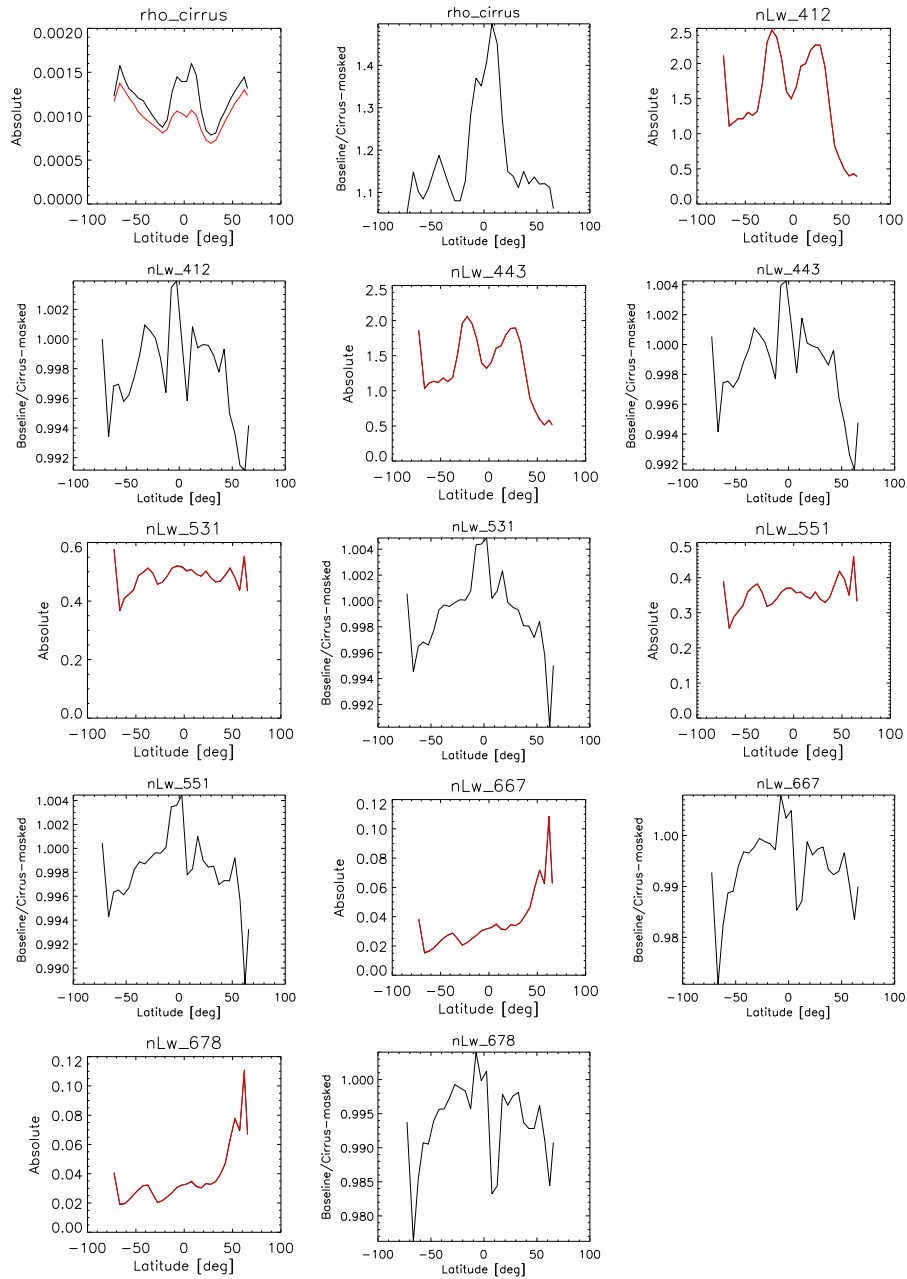


Figure 23: Different ocean color products as a function of latitude, globally averaged from the monthly level 3 files (September 2005). There are two plots for each product: the first one shows the absolute values (baseline in black, cirrus-masked in red), the second shows the ratio (baseline divided by cirrus-masked). In many cases, the red line is exactly on top of the black line in the plots of the absolute values.

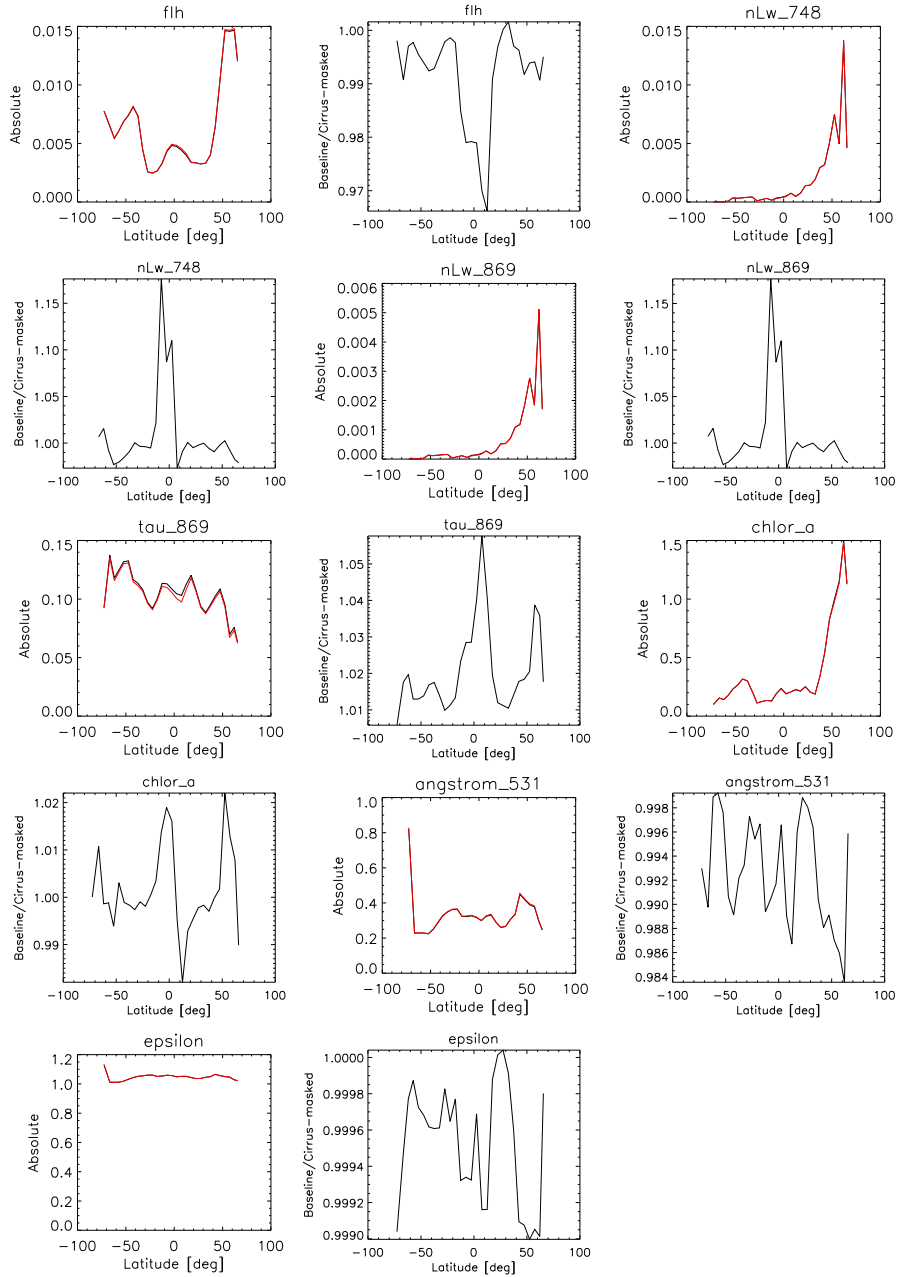


Figure 24: Different ocean color products as a function of latitude, globally averaged from the monthly level 3 files (September 2005). There are two plots for each product: the first one shows the absolute values (baseline in black, cirrus-masked in red), the second shows the ratio (baseline divided by cirrus-masked). In many cases, the red line is exactly on top of the black line in the plots of the absolute values.

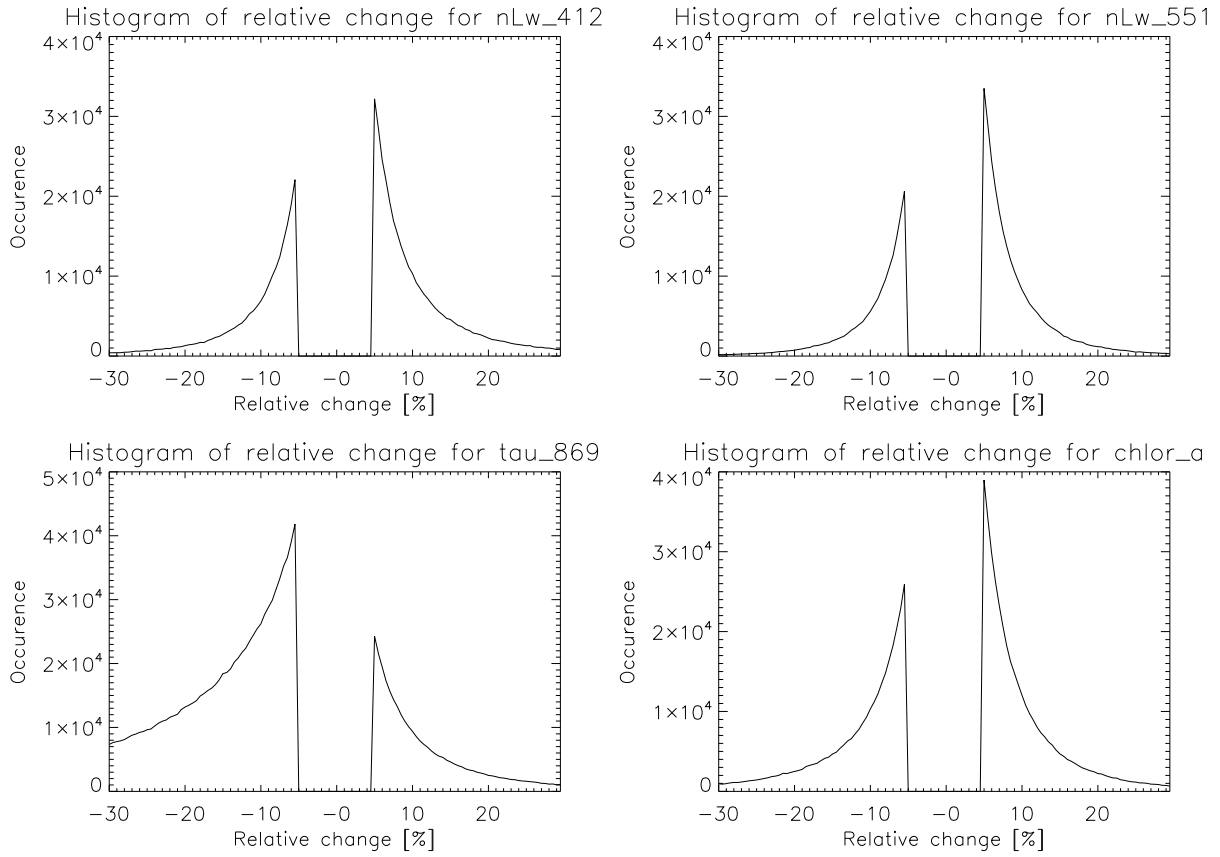


Figure 25: Histograms of the relative change (cirrus masked minus baseline) for 4 selected products from the monthly level 3 files with absolute changes larger than 5%. Histogram-binsize is 0.5%. E.g. for nLw at 412nm, there are about 6000 bins where the nLw of the cirrus masked product is lower than in the baseline product between 5.0% and 5.5%, and about 9000 bins where the cirrus masked product is higher between 5.0% and 5.5%. The vertical lines at the  $\pm 5\%$  lines are plotting artifacts.

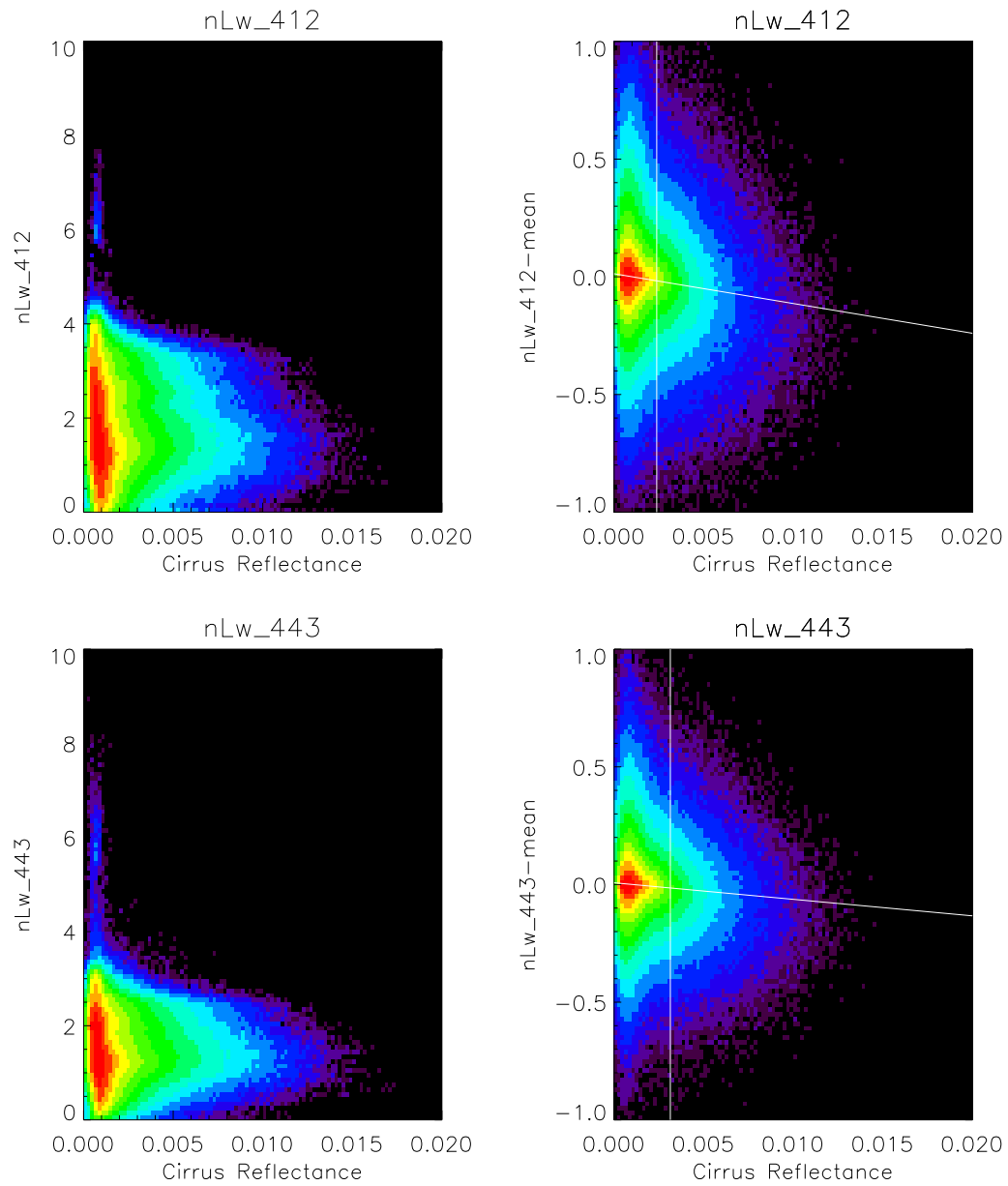


Figure 26: Scatter plot for unmasked monthly level 3 file of nLw at 412nm (top row) and 443nm (bottom row) versus cirrus reflectance, original product (left) and original product minus median median (right). The color coding is logarithmic, with purple spots being 1 bin count. The (close to) horizontal white line in the plots on the right is the linear fit (see eq. 1), the vertical white line is where the fit exceeds 1% of the mean product value.

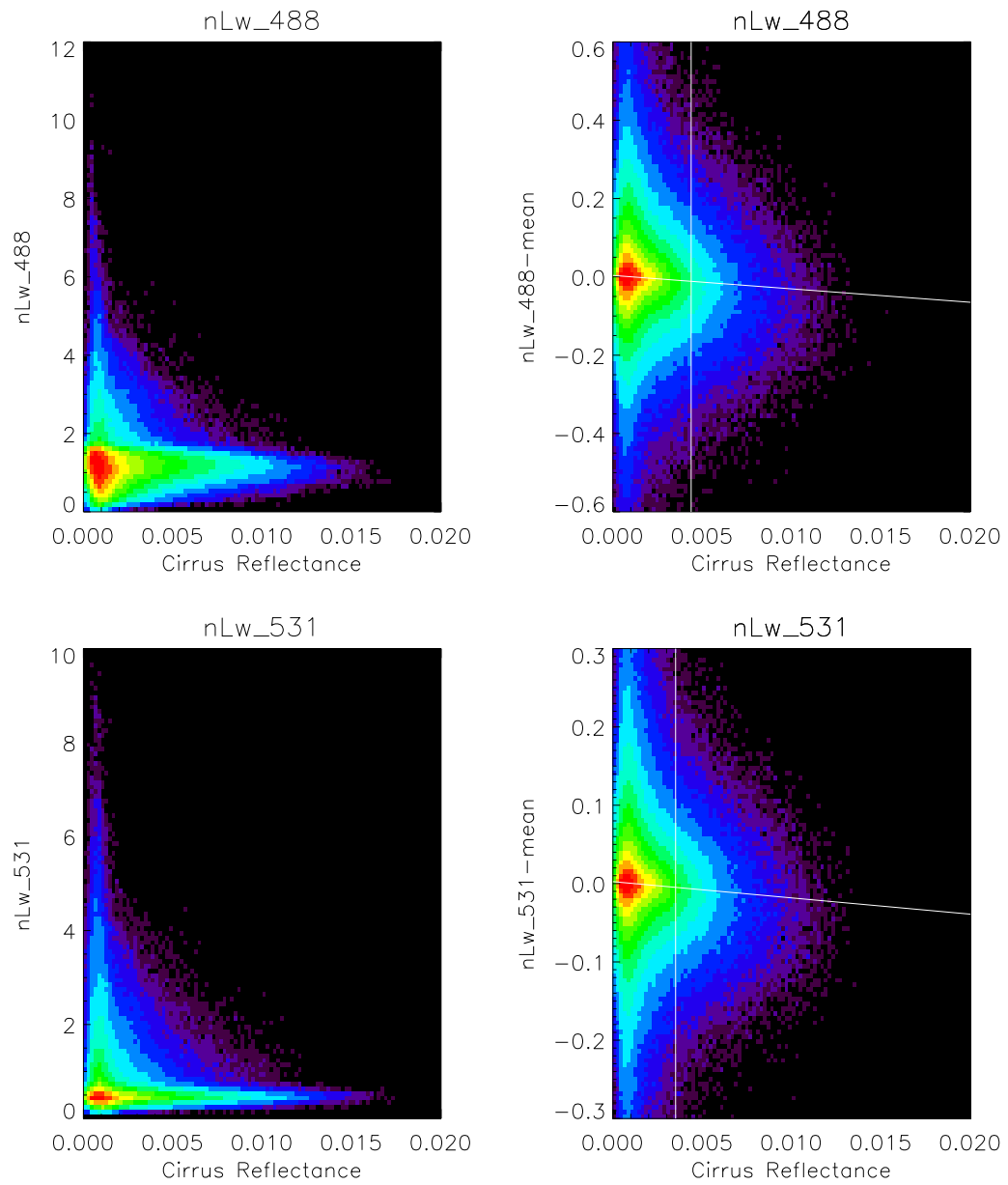


Figure 27: Same as Fig. 26 for nLw at 488nm (top row) and 531nm (bottom row).

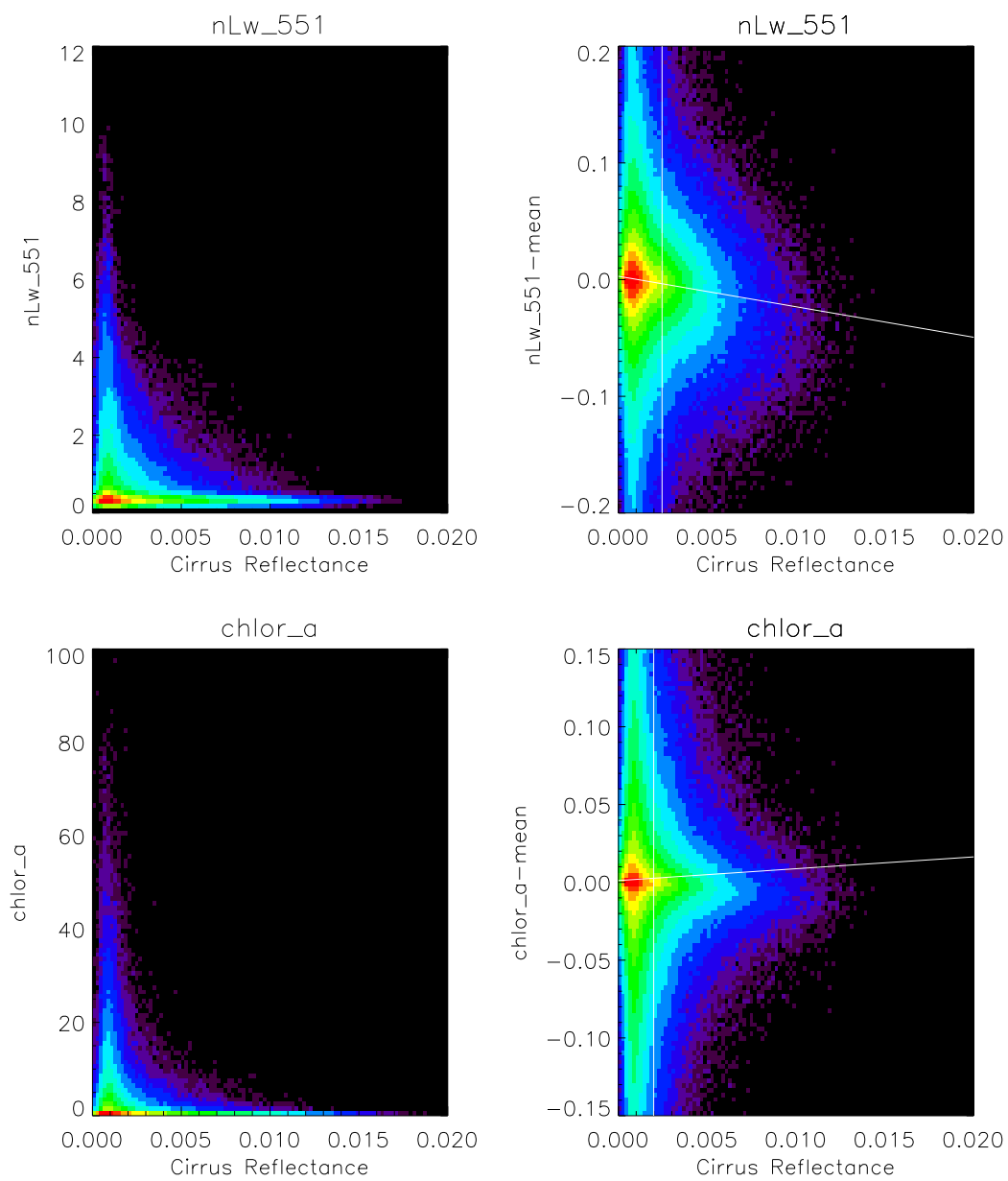


Figure 28: Same as Fig. 26 for nLw at 551nm (top row) and chlorophyll-a (bottom row). The fit to the chlorophyll data is probably distorted by outliers.

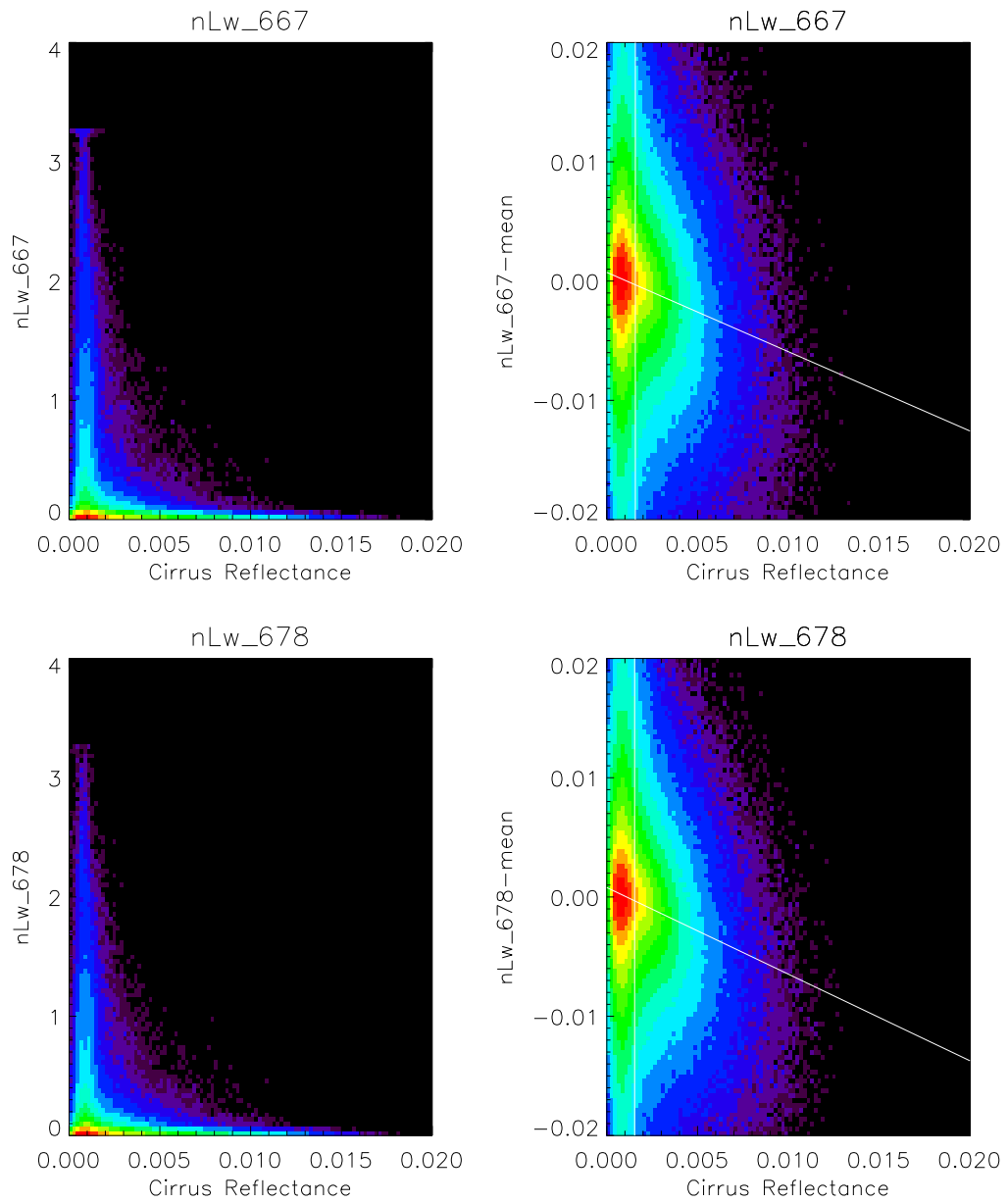


Figure 29: Same as Fig. 26 for nLw at 667nm (top row) and 678nm (bottom row).

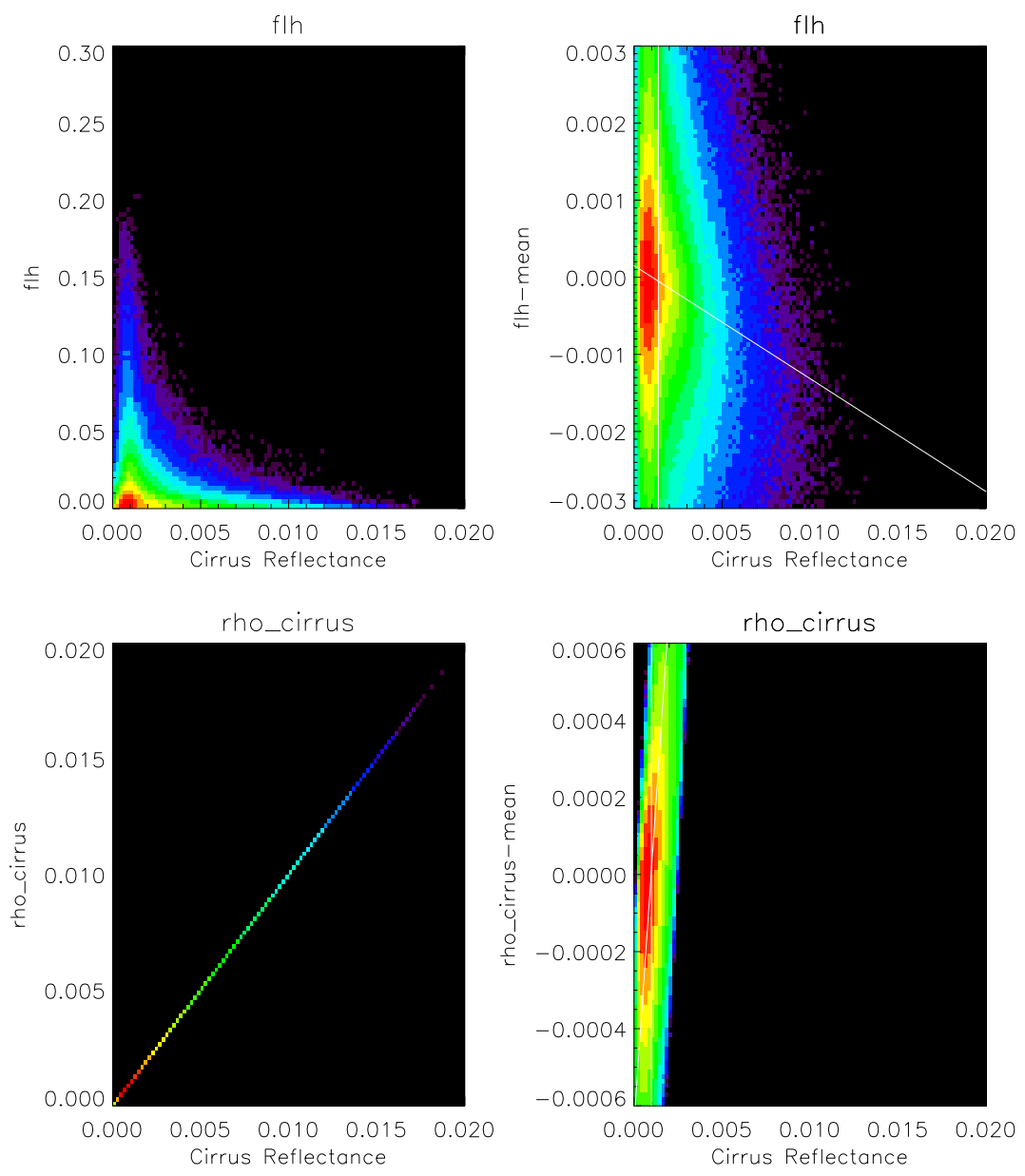


Figure 30: Same as Fig. 26 for FLH (top row) and rho-cirrus (bottom row).

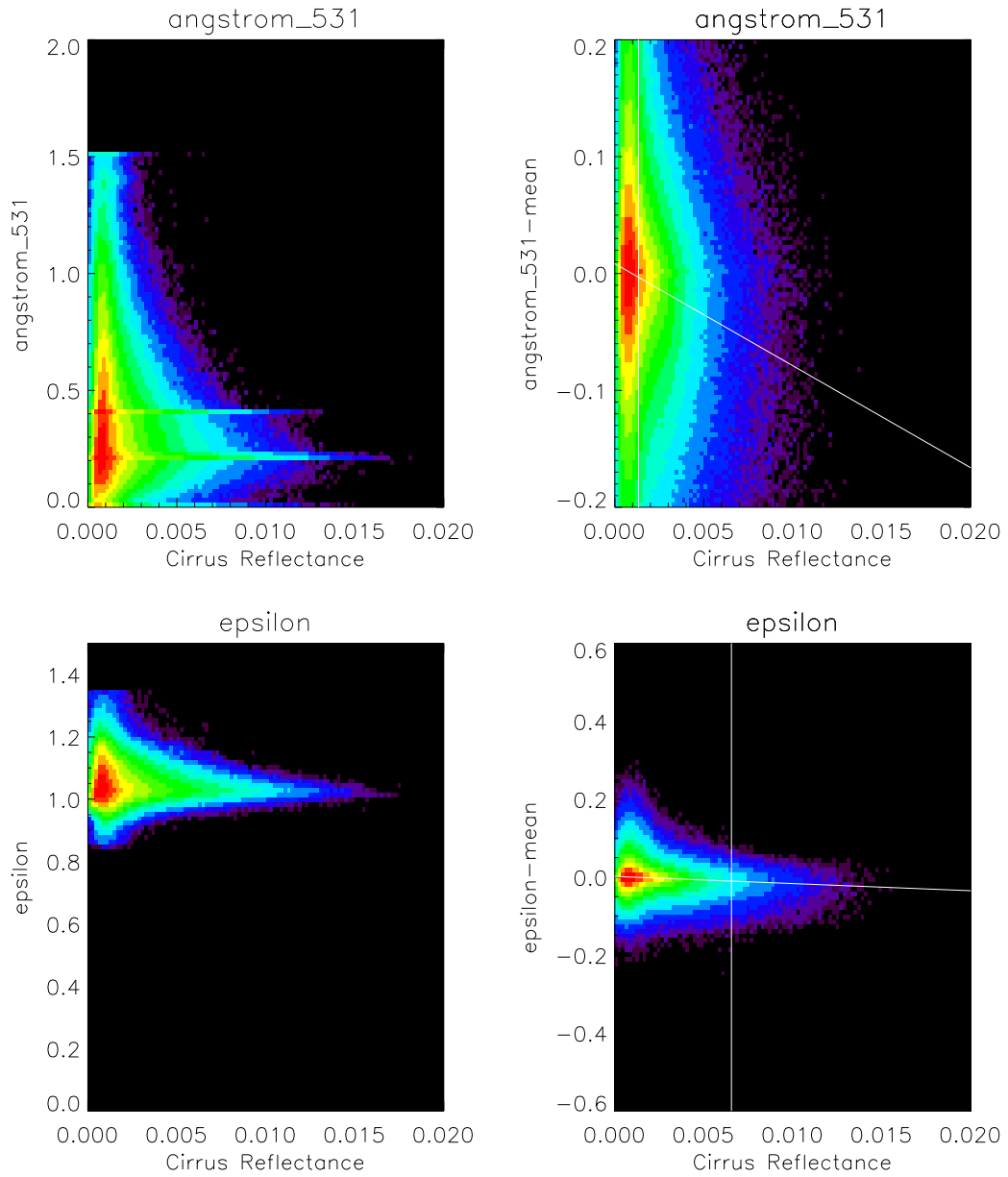


Figure 31: Same as Fig. 26 for Angstrom at 531nm (top row) and epsilon (bottom row).

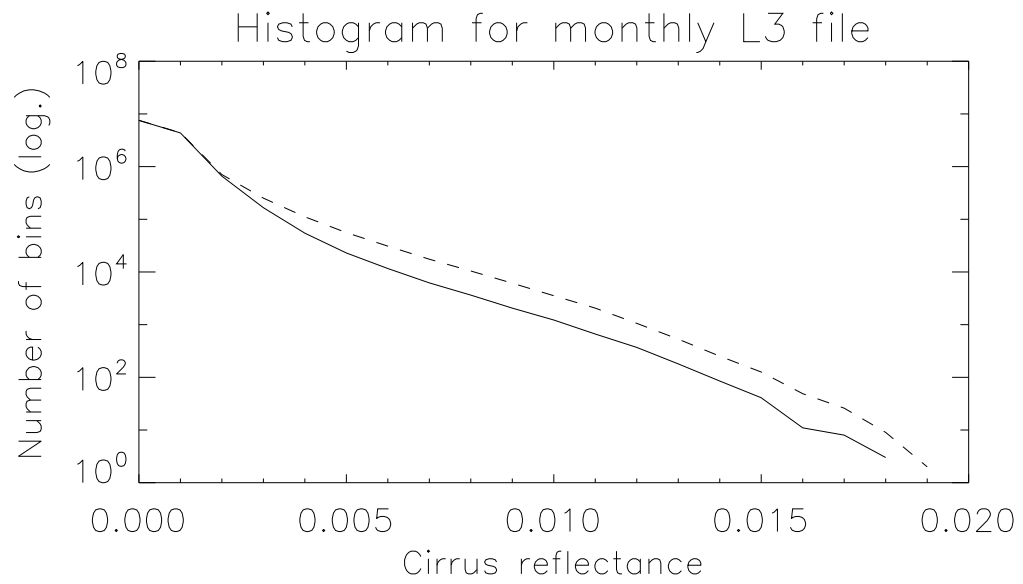


Figure 32: Histogram for cirrus reflectance in monthly L3 file (unmasked), with binsize of 0.001. Dashed line is for all bins, solid line for bins where median was calculated (i.e. all bins used in Fig. 26 to 31).